Aus der

Klinik für Allgemein-, Viszeral- und Transplantationschirurgie

Klinikum der Ludwig-Maximilians-Universität München

Vorstand: Prof. Dr. Jens Werner

The Vitamin D analogue calcipotriol attenuates pancreatic cancer malignancy via downregulating thrombospondin 1 in pancreatic stellate cells

Dissertation

zum Erwerb des Doktorgrades der Medizin

an der Medizinischen Fakultät der

Ludwig-Maximilians-Universität zu München

vorgelegt von

Chun Zhang

aus Jiangsu, Volksrepublik China

2021

Mit Genehmigung der Medizinischen Fakultät

der Universität München

Berichterstatter:	Prof. Dr. Jens Werner
Mitberichterstatter:	PD Dr. Helga Török Prof. Dr. Stefan Böck
Mitbetreuung durch den promovierten Mitarbeiter:	PD Dr. Jan G. D'Haese
Dekan:	Prof. Dr. med. dent. Reinhard Hickel
Tag der mündlichen Prüfung:	15.07.2021

LMU LUDWIG-MAXIMILIANS-UNIVERSITÄT MÜNCHEN

Dean's Office
Medical Faculty

MMRS

Affidavit

Zhang, Chun

Surname, first name

Street

Zip code, town

Germany

Country

I hereby declare, that the submitted thesis entitled

The Vitamin D analogue calcipotriol attenuates pancreatic cancer malignancy via downregulating thrombospondin 1 in pancreatic stellate cells

is my own work. I have only used the sources indicated and have not made unauthorized use of services of a third party. Where the work of others has been quoted or reproduced, the source is always given.

I further declare that the submitted thesis or parts thereof have not been presented as part of an examination degree to any other university.

Munich,26/07/2021 — Zhang, Chun

Place, date — Signature doctoral candidate

I. Table of Contents

II. Abbreviation List

°C	Degree Celsius
%	Percentage
αSMA	α-smooth muscle actin
Acr	Acrylamide
AmB	Amphotericin B
Ang-II	Angiotensin II
APS	Ammonium persulfate
ASIR	Age-standardized incidence rate
ASMR	Age-standardized mortality rate
ATRA	All-trans retinoic acid
bFGF	Basic fibroblast growth factor
BSA	Bovine serum albumin
Cal	Calcipotriol
CAFs	Cancer-associated fibroblasts
caPSCs	Cancer-associated pancreatic stellate cells
CD47	Cluster of Differentiation 47
CM	Conditioned medium
cpPSCs	Chronic pancreatitis-associated pancreatic stellate cells
CP	Chronic pancreatitis
CRC	Colorectal cancer
CT	Threshold cycle
DAB	3,3’-diaminobenzidine

DCs	Dendritic cells
DIW	Deionized water
DMSO	Dimethyl sulfoxide
ECM	Extracellular matrix
ELISA	Enzyme-Linked ImmunoSorbent Assay
EMT	Epithelial-mesenchymal transition
FAK/β1 integrin	β1 integrin-focal adhesion kinase signaling
FBS	Fetal bovine serum
Gly	Glycine
GEM	Gemcitabine
GEPIA	Gene expression profiling interactive analysis
GBSS	The Gey's balanced salt solution
GTEx	Genotype-tissue expression
h	Hour
HA	hyaluronic acid
HSCs	Hepatic stellate cells
HRP	Horseradish peroxidase
ICC	Immunocytochemistry
IL	Interleukin
mL	Milliliter
min	Minutes
mAb	Monoclonal antibody
MMP	Matrix metalloproteinase

μm	Micrometer
μL	Microliter
μg	Microgram
NEAA	Non-essential amino acids
nm	Nanometer
nM	Nanomolar
nPSCs	Normal pancreatic stellate cells
OS	Overall survival
OSCC	Oral squamous cell carcinoma cells
PAGE	Polyacrylamide gel electrophoresis
PBS	Phosphate-buffered saline
PCN	Penicillin
PCCs	Pancreatic cancer cells
PDAC	Pancreatic ductal adenocarcinoma
PDGF	Platelet derived growth factor
PFS	Progression-free survival
PSCs	Pancreatic stellate cells
qRT-PCR	Quantitative real-time polymerase chain reaction
rTHBS1	Recombinant Thrombospondin 1
RT	Room temperature
s	Second
SD	Standard deviation
SDS	Sodium dodecyl sulfate

SDF-1	Stromal cell-derived factor 1
SHH	Sonic hedgehog
SSc	Systemic sclerosis
STAT3	Signal transducer and activator of transcription 3
STR	Streptomycin
Tregs	T regulatory cells
TAMs	Tumor-associated macrophages
Th2	T helper type 2
TCA	Tricarboxylic acid
TCGA	The cancer genome atlas
THBS1	Thrombospondin 1
TGF-β1	Transforming growth factor-β1
TME	Tumor microenvironment
TNF-α	Tumor necrosis factor-α
VD	Vitamin D3
VDR	Vitamin D3 receptor
V	Volt
VEGF	Vascular endothelial growth factor
WB	Western blot
WH	Wound healing

1. Introduction

Pancreatic cancer is one of the deadliest gastrointestinal cancers with dismal clinical outcomes worldwide [1], and the majority of pancreatic cancer (around 85%) is pancreatic ductal adenocarcinoma (PDAC) [2, 3]. PDAC is characterized by the severe stromal/desmoplastic reaction in the tumor microenvironment (TME) [4-6]. Many studies have proved that the activated pancreatic stellate cells (PSCs) induce this profibrotic reaction in PDAC by modulating the production of extracellular matrix (ECM) proteins and other molecules in TME. Additionally, the interaction among PSCs, cancer cells and other stromal cells contributes to a tumor-supportive TME, thereby increasing the aggressiveness of PDAC through several signaling pathways. Recently, PSCs-targeted strategies have become promising for PDAC therapy, and several stroma-targeting strategies have been proposed [6, 7]. Among the proposed strategies, ligands of Vitamin D receptor (VDR) have emerged as a promising treatment since they have shown anti-fibrosis and TME-remodeling abilities in many diseases [8-12].

1.1 Epidemiology of pancreatic cancer

Based on data from the International Agency for Research on Cancer's GLOBOCAN, pancreatic cancer is the 11th most common cancer with 458,918 new cases and the 7th major cause of cancer-related deaths with 432,242 deaths globally in 2018 [13].

There are significant differences in age-standardized incidence rates (ASIR) and mortality rates (ASMR) among different areas, as indicated in Figure 1 [13, 14]. ASIR of pancreatic cancer is much higher in developed countries. Europe (7.7 per 100,000) and North America (7.6 per 100,000) show the highest ASIR of pancreatic cancer, while Africa (2.2 per 100,000) and South-Central Asia (<2.0 per 100,000) have the lowest ASIR [13, 15]. In addition, men have a higher ASIR of pancreatic cancer than women worldwide since pancreatic cancer is the 12th most common cancer in men and the 11th in women [13].

Although people are becoming more aware of pancreatic cancer risk factors and have developed novel tools for early diagnosis, the incidence of pancreatic cancer has climbed in recent years and is projected to rise continuously. It is estimated that there will be 355,317 new diagnoses of pancreatic cancer until 2040 [13]. In addition, pancreatic cancer is expected to overtake breast cancer soon in the European Union as the 3rd most common cause of cancer-related deaths [16].

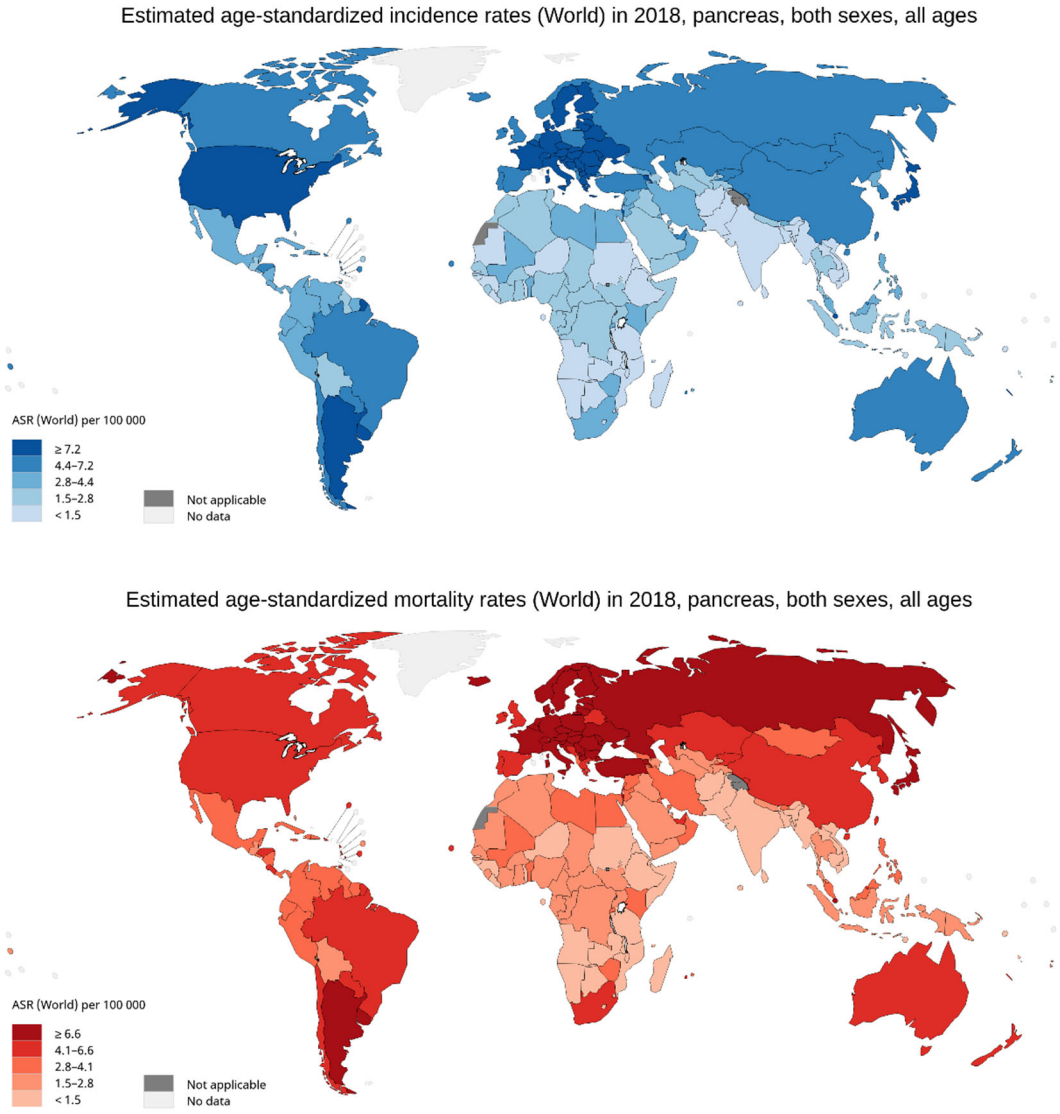

Figure 1: Maps of ASIR (up) and ASMR (down) of pancreatic cancer worldwide in 2018 (created and adjusted based on Global Cancer Observatory [14]).

1.2 Major cellular players in PDAC-TME

In the past few decades, scientists have revealed the critical role of TME in PDAC progression. TME means the crosstalk between PCCs and their surroundings, establishing a complex tumor-supportive environment for the development of PDAC. The fibrotic TME can provide a protective barrier for chemotherapy treatment and contribute to epithelial to mesenchymal transition (EMT), and allow PCCs to spread to adjacent tissues [17]. This procedure includes continuous stromal reprogramming and the activation of various pathways in PDAC-TME [18, 19]. The following parts will introduce some of the main cellular components of TME.

1.2.1 PSCs

Stellate cells were first discovered in the liver by the German anatomist Karl Wilhelm von Kupffer and described in a research letter in 1876 [20]. Nearly one century later, Wateari et al. identified similar star-shaped cells (later known as PSCs) with Vitamin A storage in mouse pancreas [21]. However, the field of PSCs didn't receive great attention until two landmark articles outlined the in vitro isolation and culture methods of PSCs in 1998 [22, 23]. With the great efforts made by many scientists, PSCs are well recognized as the significant component of fibrosis in pancreatic diseases such as chronic pancreatitis (CP) and PDAC [4, 24-26].

In health, PSCs are in a quiescent status (qPSCs) with numerous lipid droplets and can be found in the peri-acinar areas [22, 23]. qPSCs comprise around 4% of the local cells in the pancreas [27] and participate in the vitamin A storage, immunity, normal exocrine and endocrine secretion, and the maintenance of normal architecture of the pancreas [28]. Desmin, glial fibrillary acidic protein, vimentin, nestin, nerve growth factor, and neural cell adhesion molecule are able to identify qPSCs [7].

In PDAC and CP, qPSCs are continuously stimulated and transform into an activated state [29, 30]. During the transformation, PSCs change the morphology and function as follows: a) a myofibroblasts-like shape and loss of the vitamin A-rich lipid droplets; b) positive expression of α-smooth muscle actin (αSMA); c) upregulated secretion of various factors; d) increased migration and proliferation; e) elevated release of ECM components such as collagens, laminin, hyaluronic acid (HA) and fibronectin [29, 30]. In addition, the interaction of PSCs, PCCs, and other stromal cells plays a vital role in immune tolerance, chemoresistance, angiogenesis, metastasis, and recurrence of PDAC.

1.2.2 Myeloid-derived suppressor cells (MDSCs)

MDSCs are defined as immature bone marrow-derived cells exerting a vital role in the immunosuppression of PDAC. MDSCs can be induced by PCCs to mobilize from the bone marrow, enter the systemic circulation, and then be recruited to TME [31]. Diaz-Montero et al. indicated that the amount of MDSCs in the peripheral blood was closely related to the clinical cancer stage and metastatic tumor burden in PDAC patients [32]. With the growth of tumor and the generation of TME-hypoxia, hypoxia-inducible factors are increased and become the crucial factors of recruiting MDSC into PDAC-TME [33]. In TME, MDSCs-released reactive oxygen species were reported to suppress T cell responses, showing an immunosuppressive function [34]. In addition, Pinton et al. reported that the crosstalk between MDSCs and T cells could induce the immunosuppression of MDSCs [35]. MDSCs secreted the programmed death protein ligand-1, upregulated by T cells-secreted interleukin (IL)-10, could cause T cell dysfunction [35]. MDSCs-secreted IL-10 and transforming growth factor-β (TGF-β) enhanced the proliferation of T regulatory cells (Tregs), mediating the immunosuppression [36].

Evidence also showed that hypoxia could induce the differentiation of MDSCs into Tumor-associated macrophages (TAMs), another critical cell type in TME, by upregulating CD45 phosphatase and downregulating signal transducer and activator of transcription 3 (STAT3) [37].

1.2.3 TAMs

As an essential cell type in the TME, macrophages display significant plasticity allowing them to perform multiple functions in the tumor progression. Macrophages can differentiate to M1 or M2 phenotypes. M1-type macrophages take part in the formation of inflammatory and fibrotic TME in the early stages. In contrast, M2-type macrophages (known as TAMs) observed in the later stages of PDAC development can induce immunosuppression of PCCs and increase tumor malignancy [38, 39]. Accumulating evidence has indicated that TAMs play an essential role in the invasion and metastasis of cancer cells [40-42]. In PDAC patients, the elevated count of M2-polarized TAMs is associated with increased lymphatic metastasis and neural invasion [43, 44]. Cytokines can recruit TAMs into TME, and TAMs also secret many factors which increase the proliferation of PCCs [45]. TAMs-released IL-10 and TGF-β can inhibit the anti-tumor immune response mediated by dendritic cells (DCs), thereby remodeling an immunosuppressive TME [46]. In addition, PCCs can induce the differentiation of macrophages into the M2 phenotypes by paracrine pathways [47, 48]. Liou et al. reported that PCCs caused the differentiation of macrophages into the M2 phenotypes by secreting IL-13 [47].

Overall, both the TME's physical barrier effect and the TME-PCCs crosstalk contribute to the development and progression of PDAC. As one of the critical cell types in PDAC-TME, PSCs have received enormous attention recently.

1.3 Role of PSCs in PDAC

As the prominent cellular component of the PDAC-TME, PSCs have received enormous attention in recent decades [49-61]. Accumulating evidence has shown that the crosstalk among PSCs, PCCs, and other stromal cells can remodel a tumor-supportive microenvironment of PDAC, thus enhancing tumor progression and chemoresistance via various pathways [62-64]. The following sections will give a general review of the role of PSCs in PDAC progression. Figure 2 is a graphic summary of the PSCs transformation and the crosstalk among PSCs, PCCs, and other stromal cells [65].

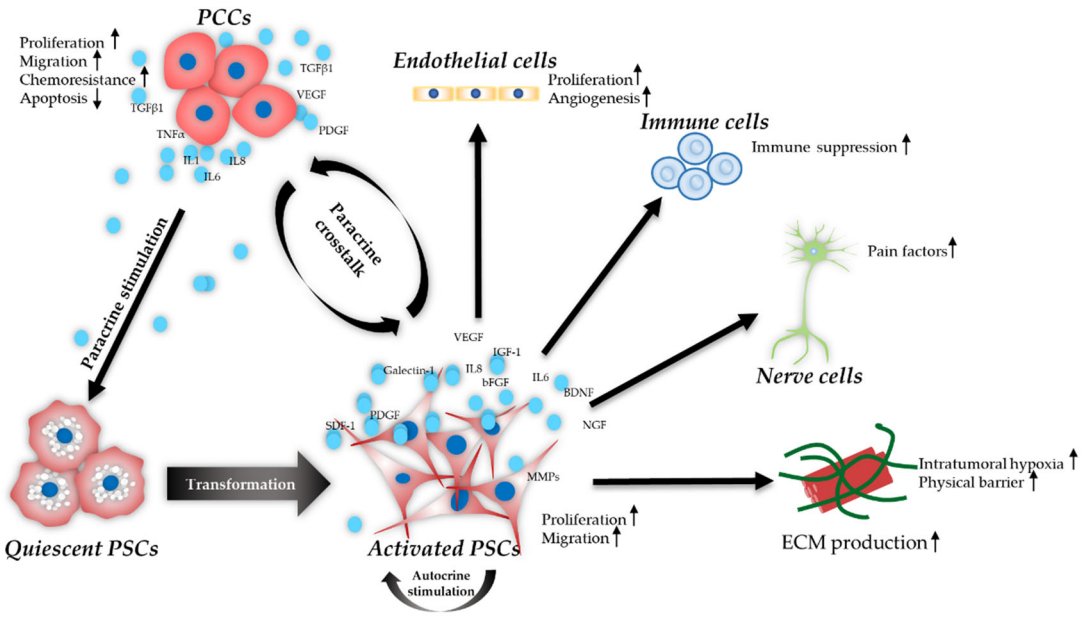

Figure 2: Simplified graph of PSCs transformation and the interaction of PSCs, PCCs, and other stromal cells (adjusted based on our review in Front. Oncol [65]). PCCs stimulate the conversion of PSCs from quiescence to an activated state by releasing chemokines or cytokines. In addition, PSCs secret numerous factors that keep PSCs continuously activated by autocrine ways and increase PCCs malignancy by paracrine

pathways. Moreover, PSCs contribute to increased angiogenesis via interacting with endothelial cells. PSCs also secret neurotrophic factors, leading to pain in PDAC. Furthermore, PSCs play an essential role in creating an immunosuppressive TME via the crosstalk with immune cells. bFGF: basic fibroblast growth factor; PDGF: Platelet-derived growth factor; VEGF: Vascular endothelial growth factor; TNF-α: tumor necrosis factor-α; MMP: Matrix metalloproteinase; SDF-1: stromal cell-derived factor 1.

1.3.1 PSCs and TME remodeling

PSCs-derived ECM components and molecules contribute to intratumoral hypoxia, EMT, angiogenesis, invasiveness, drug resistance as well as the formation of a tumor-supportive microenvironment in PDAC [66]. Berchtold et al. indicated that PSCs upregulated ECM and caused a more aggressive behavior of PCCs through β1 integrin-focal adhesion kinase (FAK/β1 integrin) signaling [67]. Di Maggio et al. indicated that ECM proteins got deposited and established a physical barrier that prevented drugs' delivery to the tumor [68]. Furthermore, deposited ECM proteins have been reported to augment interstitial pressure in tumors [69], closely correlated with vascular atrophy, hypoxia, and lack of nutrition [70].

Interestingly, some experiments showed that PSCs were able to augment the malignancy of cancer cells even in the nutrient-exhausted and hypoxic microenvironment of PDAC via paracrine signaling pathways or genetic alterations [71, 72]. For instance, upregulation of sonic hedgehog (SHH) induced by oncogenic KRAS mutations in PDAC cells can activate PSCs in the paracrine pathway. This, in turn, stimulates the PI3K-AKT signaling and respiratory activity in the mitochondria of cancer cells, thereby augmenting oxygen availability for PCCs in the hypoxic TME [73]. In addition, micropinocytosis supported by KRAS alterations enables the repurposing of

extracellular proteins for the lysosomal-mediated catabolism, which guarantees amino acids recycling and fuels tumor growth [70]. Moreover, PSCs autophagy can induce alanine production, which fuels the tricarboxylic acid (TCA) cycle in PDAC, thereby promoting non-essential amino acids (NEAA) and lipid biosynthesis [72]. Zhao et al. found that PSCs-derived exosomes contained lots of amino acids, lipids, and TCA cycle intermediates, thereby fueling PCCs for central carbon metabolism, promoting tumor growth under nutrient-deprived TME [74].

1.3.2 PSCs and drug resistance

Recent findings have revealed that PSCs can influence the drug resistance of PCCs. PSCs show a drug-scavenging ability that entraps active gemcitabine (GEM) within the stroma, making GEM unavailable for cancer cells [75]. Buckway et al. indicated that hyaluronidase treatment could enhance the penetration of chemotherapy drugs by breaking down the stromal barrier in tumor-bearing mice [76].

Furthermore, PSCs can produce various factors which enhance the resistance to drugs in PDAC [52, 70, 77]. Several studies have explored the function of PSCs in the therapeutic resistance of PDAC. Liu et al. found that PSCs-derived periostin kept the continuous activation state of PSCs, increased drug resistance to GEM, and promoted the aggressiveness of PCCs through ERK1/2 and FAK/AKT signaling [78]. Singh et al. reported that SDF-1 released by PSCs could increase the chemoresistance of PCCs via its receptor CXCR4 on cancer cells [79]. Additionally, PSCs-derived SDF-1α was reported to increase drug resistance to GEM through ERK1/2 and FAK/AKT pathways in PCCs [80]. Amrutkar et al. reported that PSCs-secreted fibronectin augmented the drug resistance of PCCs through ERK1/2 signaling [81]. Furthermore, Richards et al. showed that exosomes secreted by PSCs caused GEM resistance in cancer cells by transmitting the mRNA of Snail and miR-146a [82].

1.3.3 PSCs in PDAC metastasis

PSCs and PSCs-derived factors have been proved to play a critical role in PDAC metastasis. PSCs were shown to stimulate the EMT process in PCCs, a recognized process of initiation of PDAC metastasis [83, 84]. Neesse et al. showed that PSCs augmented the invasiveness of serine protease inhibitor nexin2 (SERPINE2)-expressing PCCs in PDAC xenograft tumors [85]. The investigations by Tian et al. indicated that PCCs could be induced into a more invasive phenotype by the binding of PCC-derived fibroblast growth factor (FGF) to its receptor on PSCs [86].

PSCs can also migrate to metastatic sites together with PCCs, forming a niche for the metastasis of PDAC. A hallmark study by Xu et al. indicated that PSCs from the primary tumor area could be even detected and further lead to a severe stromal reaction in the distant metastatic nodules, thereby creating a metastasis-supportive TME [87]. Suetsugu et al. found that after splenic injection of PSCs and PCCs, both types of cells were observed in metastatic sites by tracking PSCs expressing green fluorescence protein (GFP) [88]. All these findings further support the "seed and soil" theory regarding cancer metastasis, which was first proposed in 1889 [89]. Therefore, a recent review by Pang et al. recommended testing circulating PSCs together with circulating tumor cells as potential biomarkers in PDAC [90].

In addition, PSCs-secreted molecules have been shown to contribute to PDAC metastasis. SDF [91], galectin-3 [92], hepatocyte growth factor (HGF) [93], IL-6) [94], thrombospondin-2 [95], matrix metallopeptidase 2 (MMP2) [96] and nerve growth factor (NGF) [97] have been well proved to drive the metastasis of PDAC. A recent study by Schnittert et al. indicated that integrin α11 was upregulated in PSCs activation and increased PDAC metastasis [98]. Another study by Qian and his colleagues demonstrated that PSCs upregulated galectin-1 and enhanced the invasiveness of

PCCs by paracrine SDF-1 [99]. Apte's team revealed that PSCs-secreted HGF enhanced the aggressiveness of PDAC via its receptor c-MET on cancer cells, and HGF inhibition resulted in a significant reduction of metastasis in a mouse model of PDAC [100, 101]. As such, PSCs and PSCs-secreted factors need more attention in the future development of therapeutics for PDAC.

1.3.4 PSCs and immune suppression

PDAC is also characterized by the evasion of host immune surveillance, and several studies have indicated that PSCs also play a significant role in this process [102-105]. Ene-Obong et al. demonstrated that PSCs-derived SDF-1 showed a chemotactic effect on $CD8^+$ T cells, thereby hampering their infiltration into tumor areas [106]. Wu et al. indicated that PSCs upregulated the secretion of TGF-β1 and IL-10, which exposed inhibitory impacts on DCs and led to immune suppression in pancreatic cancer [107]. Furthermore, two studies demonstrated that PSCs induced the differentiation and expansion of MDSCs by the IL-6/STAT-3 pathway, thus creating an immunotherapy-resistant microenvironment [70, 108]. The work by Tang et al. revealed that PSCs-secreted galectin-1 impeded the activation of T cells, induced their apoptosis, and increased the secretion of T helper type 2 (Th2), thus forming an immunosuppressive TME of PDAC [102]. Lunardi et al. demonstrated that PSCs-secreted IL-10 improved recruitment of CXCR3+ Tregs and reduced cytolysis intermediated by T-cells and NK-cells, thereby causing the immunosuppressive and tumor-promoting effects [109].

Overall, PSCs play a vital role in the immune response against PDAC by various pathways. Restoring the immune reaction against PCCs by targeting PSCs is promising for improving the clinical outcomes of PDAC patients.

1.3.5 PSCs and angiogenesis in PDAC

In PDAC, PSCs can secret many pro-angiogenic factors, such as VEGF, bFGF, IL-8, PDGF, and periostin, which promote proliferation, survival, and migration of endothelial cells, thereby contributing to angiogenesis [110]. Tang et al. found that prokineticin (PK) secreted by aPSCs promoted angiogenesis by inducing the function of the PK/PKR system on endothelial cells [110]. Kuninty et al. showed that TGF-β-activated PSCs induced tube formation (a measure of angiogenesis) of endothelial cells, which could be regulated via the therapeutic miRNA-199a-3p and miRNA-214-3p [111]. Patel et al. showed that PSCs increased proliferation and tube formation of microvascular endothelial cells via the HGF/c-Met pathway [112].

1.3.6 PSCs and nerve interaction in PDAC

PSCs are also involved in neural invasion in PDAC. Li et al. demonstrated that activated PSCs induced neurite outgrowth towards PCCs and promoted the neural invasion of PCCs [113]. More recently, Nan et al. reported that PSCs promoted the perineural invasion of PCCs via the HGF/c-Met pathway [59]. In addition, Han et al. reported that PSCs contributed to pain in PDAC by PSCs-induced secretion of pain factors from dorsal root ganglia [114]. Demir et al. also found that conditioned medium (CM) from cancer-associated PSCs could stimulate neuron outgrowth [115].

In summary, PSCs contribute to the severe stromal/desmoplastic reaction in PDAC-TME. In addition, the PSCs-PCCs paracrine crosstalk remodels a tumor-supportive stroma which increases the malignancy of cancer cells. Recently, targeting PSCs has emerged as a promising strategy for PDAC therapy, and several targeted therapies have been proposed.

1.4 Therapeutic strategies targeting PSCs

Due to the increasingly recognized role of the PSCs in PDAC progression, some approaches to modulate the tumor stroma have been developed [51, 78, 99, 111, 116-118]. Among these strategies, simple PSCs depletion was shown to cause more aggressive tumors with decreased survival in the transgenic mouse model of PDAC [119]. Consequently, recent studies have focused on normalizing PSCs or reducing ECM directly [120-123]. Figure 3 is a schematic diagram of the leading strategies, and the following sections will review several novel promising approaches.

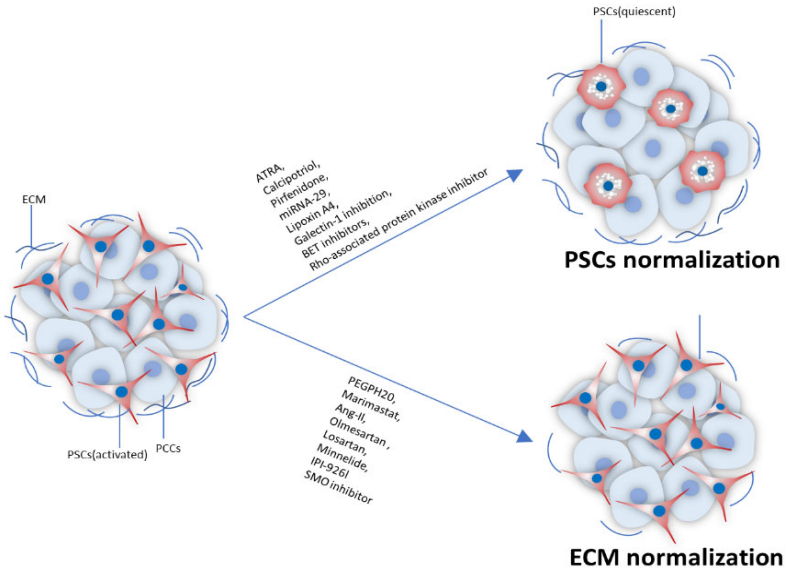

Figure 3: Principal strategies for PSCs-directed PDAC treatment. Two main strategies targeting PSCs or ECM as PDAC treatment are discussed. To begin with, PSCs can be normalized into an inactive phenotype by utilizing molecules like ATRA or calcipotriol (Cal). In addition, PSCs-derived ECM proteins can be targeted directly to induce stromal exhaustion.

i) SHH pathway inhibitors

PCCs have been shown to accelerate the stromal reaction via the paracrine SHH pathway [114]. Experiments on inhibiting SHH signaling showed different results. Oliver et al. demonstrated that a combination of IPI-926 (a hedgehog inhibitor) and GEM enhanced the intratumoral vascular density and GEM delivery to the tumor [124]. Nevertheless, Rhim and his colleagues indicated that PDAC mice with SHH deletion displayed more aggressive and undifferentiated tumors than controls [125]. Hence, the phase II clinical trial based on IPI-926 was canceled on account of elevated mortality [126]. Hwang et al. indicated that AZD8542 (a novel hedgehog inhibitor) decreased tumor volume and metastasis in an orthotopic model of PDAC [127].

ii) Vitamin A analogs

Vitamin A analogs show an ability to normalize PSCs. For instance, after treatment of PSCs with all-trans retinoic acid (ATRA), activation of PSCs was prevented, resulting in less aggressiveness of PCCs by paracrine signaling [123, 128, 129]. Moreover, Han et al. demonstrated that gold nanoparticles containing ATRA and heat-shock protein 47 siRNA normalized PSCs, resulting in increased intratumoral GEM concentration [130]. Nevertheless, several clinical trials with vitamin A analogs exhibited unsatisfactory results. Michael et al. showed that combination therapy with GEM and 13-cis-retinoic acid (13-cis-RA) could not improve the response rate in PDAC patients [131]. Moore et al. indicated that combination therapy (13-cis-RA+interferon-α) was not able to exhibit objective anti-cancer activity in PDAC patients [132]. Recently, another trial (NCT03307148) repurposing ATRA as a stromal targeting agent along with GEM plus nab-paclitaxel for PDAC is underway, and its phase Ib trial (NCT03307148) has shown that ATRA+GEM+nab-paclitaxel treatment in advanced, unresectable PDAC patients is safe and tolerable [133].

iii) Angiotensin II (Ang-II) Inhibitors

Two Ang-II inhibitors (olmesartan) have been investigated since Ang-II is able to increase the proliferation of PSCs via protein kinase C and EGF/ERK signaling [134]. Masamune et al. showed that Olmesartan could decrease proliferation and collagen I synthesis by PSCs, thereby reducing carcinoma growth in vivo [135]. Another study by Chauhan et al. indicated that losartan reduced intratumoral pressure and decompressed tumor blood vessels, which increased drug delivery and oxygen delivery to tumors in orthotopic PDAC mice [136].

iv) Pirfenidone

Pirfenidone, an antifibrotic agent for treating idiopathic pulmonary fibrosis, was reported to deactivate PSCs and decrease the production of collagen and periostin, thus reducing proliferation and invasion of pancreatic cancer cells in vivo [137]. Kozono et al. showed that combination therapy (pirfenidone+GEM) normalized PSCs and reduced the production of collagen, thereby decreasing tumor growth and liver metastasis in an orthotopic model of PDAC [137]. Suklabaidya et al. indicated that combination strategy (pirfenidone+N-acetyl cysteine) decreased desmoplasia as well as the growth and metastasis of tumor in an orthotopic hamster model of PDAC [138].

v) miRNA-based approaches

Recently, researchers have also tried to modulate PSCs with miRNA [139]. Kwon et al. showed that miRNA-29 was decreased when PSCs got activated, and overexpression of miRNA-29 in PSCs decreased invasiveness of PCCs in co-culture [140]. Asama et al. revealed that miRNA let-7d showed an anti-fibrosis effect by deactivating PSCs through downregulating thrombospondin 1 (THBS1) [141].

vi) Lipoxin A4 (LXA4)

Schnittert et al. unraveled that endogenous lipid LXA4 was able to inhibit pancreatic fibrosis by deactivating PSCs, thereby abolishing PSCs-induced tumor growth and invasiveness in a co-injection subcutaneous tumor model [121].

vii) Galectin-1

Qian et al. indicated that galectin-1 was overexpressed in PSCs, and knockdown of galectin-1 inhibited liver metastasis in a co-injection orthotopic PDAC model [99]. Most recently, Orozco et al. showed that deletion of galectin-1 resulted in decreased stromal activation and vascularization, improved T cell infiltration, and decreased cancer metastasis in a PDAC mouse model [142].

viii) Polyethylene glycol (PEG)ylated hyaluronidase

Jacobetz et al. found that combination therapy with GEM and PEGPH20 (a PEGylated hyaluronidase) degraded stromal HA, leading to decreased intratumoral pressure, decompression of tumor blood vessels, increased delivery of GEM, and prolonged survival in a PDAC mouse model [143]. A phase Ib trial by Hingorani et al. showed that drug combination (PEGPH20+GEM) could prolong the overall and progression-free survival (OS and PFS) rates in patients with advanced PDAC [144]. Moreover, in a phase II trial, the largest improvement in PFS was observed in patients with HA-rich tumors who received the combination therapy (PEGPH20+nab-paclitaxel+GEM) [145].

From the above, we can see that the stroma-targeted strategies have been well acknowledged. The strategies mainly focus on normalizing PSCs or reducing ECM directly have been well developed. In many diseases, Vitamin D3 (VD) analogs are well proved to show an anti-fibrosis function by targeting myofibroblasts [146-155].

1.5 Therapeutic potential of VD analogs in PDAC

Given that fibrotic stroma plays a critical role in tumor aggressiveness, repurposing VD analogs could be of great therapeutic potential in the treatment of PDAC.

A hallmark in vivo study by Sherman et al. revealed that VD analog reduced stromal fibrosis and improved the drug delivery to the PDAC tumor region [122]. Additionally, Kong et al. showed that VD analog reduced the release of exosomal miR-10a-5p by PSCs, thereby decreasing tumorigenic impacts of this oncomiRNA on PCCs [156]. Based on these studies, a clinical trial (NCT03520790) is currently ongoing to investigate the drug combination of paricalcitol, nab-paclitaxel, and GEM, in patients with metastatic PDAC [157].

Previously, our group investigated the effect of a VD analog, Cal, on the PSCs normalization and PSCs-induced malignancy of PCCs [158]. The effect of Cal on PSCs normalization was explored. Cal significantly decreased the expression of αSMA (a marker of activated PSCs) at mRNA and protein levels. In addition, Cal reduced the abilities of proliferation and migration of PSCs. These results suggested that the VD analog could decrease the activation of PSCs. Furthermore, Cal was able to significantly diminish PSCs-enhanced migration, invasion, and proliferation of PCCs, using transwell migration, invasion, and EZ4U assay, respectively.

1.6 Aim of this study

The overall objective of this study is to investigate the role of VDR in the PSCs-augmented malignancy (proliferation, migration, invasion, and EMT) of PCCs. In addition, I will further explore which molecule is involved in this crosstalk and how that molecule influences this procedure.

2. Materials and Methods

2.1 Materials

2.1.1 Apparatus

Autoclave	Unisteri, DE
BD LSRFortess™ cell analyzer	BD Bioscience, DE
Centrifuge	Heraeus, DE
Cell culture incubator	Binder, DE
Cell culture incubator	Thermo Fisher Scientific, USA
Combitips Plus	Sigma-Aldrich, USA
Centrifuge	Eppendorf, DE
ChemiDoc MP Imaging System	Bio-Rad, DE
Microcentrifuge	Labtech, DE
DNA workstation	Uni Equip, DE
Drying oven	Heraeus, DE
Digital pH-Meter	Knick, DE
Ice machine	KBS, DE
Laminar flow	Heraeus flow laboratoies, DE
Liquid nitrogen tank	MVE, USA
Microscope	Olympus, DE

Micro weigh	Chyo, DE
Microplate reader	VERSAmax, DE
Mini tran-blot electrophoretic transfer cell	Bio-Rad, DE
Multipette plus pipette	Eppendorf, DE
NanoDrop™ 2000/2000c spectrophotometer	Thermo Fisher Scientific, USA
Odyssey CLx	LI-COR, USA
Pipettes	Sigma-Aldrich, USA
Power supply PowerPac 300	Bio-Rad, DE
Shaker	Edmund Buehler, DE
StepOne real-time PCR systems	Applied Biosystems, DE
Thermocycler	Eppendorf, DE
Thermomixer comfort 5355	Eppendorf, DE
UV transilluminator	Labortechnik, DE
Vortex mixer	Labnet, DE
Waterbath	Memmert, DE
Shaking water bath	Kottermann Labortechnik, DE
X cell II Blot module	Invitrogen, DE
Fridge-freezer (4, -20, -80°C)	Siemens, DE

2.1.2 Computer Software, hardware, and website

Endnote X9	Clarivate Analytics, USA
GraphPad Prism 7	GraphPad, USA
ImageJ	National Institutes of Health, USA
SPSS statistics 21.0	IBM, USA
Hardware	HP, USA
Gene Expression Profiling Interactive Analysis (GEPIA)	http://gepia.cancer-pku.cn/index.html
STRING	https://string-db.org

2.1.3 Experimental consumables

Cell culture flasks (T25, T75, T125)	Thermo Fisher Scientific, Denmark
Corning cell scrapers	Sigma-Aldrich, DE
T.I.P.S. (10, 20, 100, 200, 1000µl)	Eppendorf, DE
Falcon cell strainer (40µm, 70µm, 100µm)	BD Bioscience, USA
15mL centrifuge tubes	TPP, Switzerland
50mL centrifuge tube	Corning, Mexico
Hyperfilm ECL	GE healthcare, DE
PVDF membrane	Sigma-Aldrich, DE
Lab gloves (green, orange)	SHIELD Scientific, Netherlands

Cell culture plates (6-, 12-, 24-, 96-well)	Thermo Fisher Scientific, Denmark
Pipette (1, 5, 10, 25, 50mL)	Costar, USA
Scalpels #22	Thermo Fisher Scientific, DE
Needles	BD Bioscience, Spain
Syringe filters (0.25, 0.45µm)	Sartorius, DE
Thick blot filter paper	Bio-Rad, DE

2.1.4 Chemical reagents and buffers

Amphotericin B (AmB) solution	Sigma-Aldrich, DE
30% Acrylamide (Acr)	Roth, DE
Ammonium persulfate (APS)	Serva, USA
Bovine Serum Albumin(BSA)	Biomol,DE
Collagenase P	Roche, DE
Crystal violet	Sigma-Aldrich, DE
$CaCl_2 \cdot 2H_2O$	Merck, DE
Calcipotriol (Cal)	Sigma-Aldrich, DE
D-(+)-Glucose	Sigma-Aldrich, DE
Dimethyl sulfoxide (DMSO)	Sigma-Aldrich, DE
Dulbecco’s modified Eagle medium (DMEM)	Gibco, USA

DMEM/F12	Gibco, USA
DNase	Roche, DE
ECL™ Western blotting system	Amersham Biosciences, DE
Ethanol (70%, 96%, >99%)	Apotheke GH, DE
Fetal bovine serum (FBS)	Sigma-Aldrich, DE
Glycine (Gly)	Roth, DE
Isopropanol	Roth, DE
KCl	Serva, DE
KH_2PO_4	Sigma-Aldrich, DE
2-Mercaptoethanol	Sigma-Aldrich, DE
Mouse IgG1 Isotype Control	NOVUS, DE
$MgCl_2 \cdot 6H_2O$	Fluka, Switzerland
$MgSO_4 \cdot 7H_2O$	Merck, DE
Milk powder	Roth, DE
$NaHCO_4 \cdot 2H_2O$	Merck, DE
$NaHCO_3$	Sigma-Aldrich, DE
NaCl	Sigma-Aldrich, DE
Nycodenz	Axis-shield PoC, Norway
Phosphate-buffered saline (PBS)	PAN-Biotech, DE
Penicillin-Streptomycin (PCN-STR) Mixture	Lonza, USA

Pronase	Roche, DE
Standard proteins	Bio-Rad, USA
Protease inhibitor cocktail	Roche, DE
Recombinant Human THBS1 (rTHBS1)	NOVUS, DE
RPMI media 1640	Gibco, USA
RNase-free water	Qiagen, DE
RIPA lysis buffer, 10X	Millipore, DE
Sample buffer, 4X	Bio-Rad, USA
Sodium dodecyl sulfate (SDS)	Roth, DE
Trypan blue	Sigma-Aldrich, DE
TEMED	Bio-Rad, USA
Triton-X-100.	Sigma-Aldrich, Switzerland
Trypsin/EDTA solution	Lonza, Switzerland
Tris	Bio-Rad, USA
Tween 20	Sigma-Aldrich, DE
Versene Solution	Gibco, USA

2.1.5 Kits and Primers

BCA protein assay kits	Thermo Fisher Scientific, DE

cDNA Synthesis kits	Bio-Rad, USA
Matrigel matrix	Corning, DE
QuantiTect Reverse Transcription Kit	Qiagen, DE
QuantiTect Primer Assays	Qiagen, DE
RNeasy Micro Kit	Qiagen, DE
Transwell Inserts, Polyester membrane	Corning, DE
EZ4U kit BI-5000	Biomedica, Austria
Human THBS1 Quantikine ELISA Kit	R&D systems, DE
Vimentin primer	Qiagen, DE
E-cadherin primer	Qiagen, DE
N-cadherin primer	Qiagen, DE
GAPDH primer	Qiagen, DE

2.1.6 Antibodies

Antibody	**Source**
CD47 antibody	NOVUS, DE
GAPDH (D16H11) XP Rabbit mAb	CST, DE
Thrombospondin-1 antibody (A6.1)	NOVUS, DE
IRDye (800CW, 680RD) Secondary Ab	LI-COR, USA
Rabbit anti-Sheep Secondary Ab	NOVUS, DE

2.2 Methods

2.2.1 Primary PSCs Isolation and Culture

Activated PSCs used in this project included PSCs from PDAC tumor tissue or CP fibrotic tissue. These PSCs were isolated by the outgrowth approach [23] utilizing pancreatic tissues from PDAC or CP patients who underwent surgical resection in our hospital. Tissues were obtained from the Biobank of our department and had already been anonymized before research. The Biobank had already got the informed consent of the patients and ethical approvement. For the isolation of activated PSCs, tissues were firstly removed of adipose and connective parts and washed by PBS. Tissues were then cut into small pieces (0.5-1mm^3). Subsequently, tissue pieces were cultivated in 6-well plates (around 5-10 fragments/well). DMEM/F12, including 20% FBS, was used as the culture medium, and the formula could be found in Table 1. The plates containing tissue fragments were maintained in an incubator under standard culture conditions (37°C, 5% CO_2/air, humid environment), and the media was renewed after 24h. After 3-5 days, activated PSCs grew from the edge of tissue fragments and could be observed under a light microscope. After PSCs reached a confluence of around 20%, tissue pieces were then removed, and the medium was refreshed twice a week. PSCs were collected and kept in a liquid nitrogen tank after they reached an 80% confluence.

qPSCs were isolated via the method called density gradient centrifugation created by Apte's team [22, 159]. Briefly, adjacent normal pancreas tissues were obtained from patients with pancreatic diseases who underwent surgical resection in our hospital. Following the elimination of adipose and connective parts, the tissues were sliced into fragments. Then, 20mL enzyme solution and 20μL DNase solution (formula in Table 1) were added, followed by a 15min incubation with 120 cycles/min at 37°C. Subsequently,

a cell strainer (100μm) was used to filter the solution, and the GBSS+NaCl solution (Table 1) was used to wash the nylon mesh twice. The 9.5mL BSA solution and 8mL Nycodenz solution were utilized to resuspend cells (Table 1). After a 20min centrifugation (1400g, 4°C), the fuzzy band containing qPSCs could be observed at the interface of the BSA and Nycodenz solutions mentioned above. This band was then harvested and kept in the DMEM/F12, including 20% FBS in the incubator (37°C, 5% CO2/air, humid environment). Finally, PSCs were harvested for further experiments or stored in a liquid nitrogen tank after 80% confluent.

Table 1 The formulas of different solutions involved in PSCs separation and culture

Solutions	**Chemical reagents**	**Dosage**
$MgSO_4$	$MgSO_4 \cdot 7H_2O$	700mg
	Deionized water (DIW)	0.1L
KH_2PO_4	KH_2PO_4	3000mg
	DIW	0.1L
KCl	KCl	3700mg
	DIW	0.1L
Na_2HPO_4	$Na_2HPO_4 \cdot 2H_2O$	1500mg

	DIW	0.1L
$MgCl_2$	$MgCl_2 \cdot 6H_2O$	2100mg
	DIW	0.1L
$CaCl_2$	$CaCl_2 \cdot 2H_2O$	33.4mg
	DIW	0.1L
DNase	DNase	0.01mg
	DIW	1mL
GBSS+NaCl	D-(+)-Glucose	250mg
	DIW	234.5mL
	NaCl	1750mg
	$NaHCO_3$	567.5mg
	$CaCl_2$ solution	2.5mL
	KH_2PO_4 solution	2.5mL

	KCl solution	2.5mL
	$MgCl_2$ solution	2.5mL
	$MgSO_4$ solution	2.5mL
	Na_2HPO_4 solution	2.5mL
GBSS-NaCl	D-(+)-Glucose	50mg
	DIW	47mL
	$NaHCO_3$	113.5mg
	$CaCl_2$ solution	0.5mL
	KH_2PO_4 solution	0.5mL
	KCl solution	0.5mL
	$MgCl_2$ solution	0.5mL
	$MgSO_4$ solution	0.5mL
	Na_2HPO_4 solution	0.5mL

Enzyme	Collagenase P	26mg
	GBSS+NaCl solution	20mL
	Pronase	20mg
0.3% BSA	BSA	150mg
	GBSS+NaCl solution	50mL
Nycodenz (28.7 %)	Nycodenz	2.87g
	GBSS-NaCl solution	10mL
Complete medium (20%FBS)	AmB	0.625mg
	DMEM/F12	200mL
	FBS	50mL
	PCN	$2.5x10^4$ units
	STR	25mg
Complete medium (10%FBS)	AmB	0.5mg

	DMEM/F12	180mL
	FBS	20mL
	PCN	$2x10^4$units
	STR	20mg

2.2.2 PCCs Culture

Human pancreatic cancer cell lines (PANC-1, MIA PaCa-2, AsPC-1) were initially gained from ATCC company and maintained in our lab. PDAC cell lines were thawed and cultured with RPMI-1640 medium. PCCs were cultured in the incubator (37°C, 5% CO2/air, humid environment) for further experiments. 0.025% Trypsin/EDTA solution was used for cell dissociation. Every four months, a routine test was performed to check cells for mycoplasma in accordance with the internal SOPs. Once a year, cell authentication was conducted by IDEXX BioResearch (Ludwigsburg, Germany).

2.2.3 qRT-PCR

2.2.3.1 RNA extraction

RNA extraction was conducted according to the protocol of the Qiagen RNeasy Micro Kit. Firstly, cells were washed three times with PBS and were resuspended with the 350μl RLT solution. The cell lysate was then added into columns which were set in the collection tube. The tube was centrifuged (2min, 16000g) at room temperature (RT), and 350μl ethanol (70%) was added and well mixed. The mix was added into a clean column in a new tube, which was further centrifuged (15s, 8000g, RT). The tube with

flowthrough was discarded, and 350µl RW1 solution was added to the column. After another centrifugation (15s, 8000g, RT) and elimination of flowthrough, 80µl DNase I mix was pipetted into the column for incubation (15min, RT). After that, 350µl RW1 solution was pipetted into the column, which was further centrifuged (15s, 8000g, RT). The column was rearranged into a new tube and was added with a 500µl RPE solution. After centrifugation (15s, 8000g, RT), the tube with flowthrough was discarded, and 500µl 80% ethanol was added into the column. After another centrifugation (2min, 8000g, RT) and rearrangement in a clean tube, the column was centrifugated again (5min, 16000g, RT). Subsequently, the column was rearranged in a new tube and was added with14µl RNase-free water. Following a 1min centrifugation (16000g, RT), RNA could be obtained and stored at -80°C.

2.2.3.2 Reverse transcription and cDNA pre-amplification

Reagents such as Quantiscript RT and RT Primer Mix should be maintained at RT before use, while RNA was kept in an icebox. The manufacturer's protocol was followed to remove the genomic DNA. Briefly, the tube including reagent mixture (1µL RNase-free water, 2µL Wipeout buffer, 11µL template RNA) was placed into Thermomixer at 42°C for 2min. The tube was then instantly put on ice. For reverse transcription, the tube was added with another mixture (1µl Quantiscript Reverse Transcriptase, 4µl Quantiscript RT Buffer, 1µl RT Primer Mix) for a 15min incubation at 42°C. For transcriptase inactivation, the tube was incubated for 3 min at 95°C. Ultimately, cDNA could be achieved for further tests or maintained at -20°C.

2.2.3.3 qRT-PCR procedure

In our research, the fluorescence was detected using an intercalating reagent, SYBR Green I, which could fluoresce when bounding to the double-stranded DNA. The complex of DNA and SYBR Green could be inspired at 494nm and emit green light at

520nm. The target DNA could be quantitatively determined by assessing the fluorescence. The PCR cycles include one cycle for initial denaturation (95°C, 5min), 40 cycles for primer hybridization (95°C, 10min) and elongation (60°C, 30min), and one cycle for melting (heating from 60 to 95°C in 6min). The fluorescence intensity was proportional to the PCR reaction, so it could be applied to assess the amount of the related nucleic acids. A threshold for the fluorescence intensity was established, and the threshold cycle (Ct) represented the cycle number when the fluorescence reached the threshold. For the relative quantification, the GAPDH gene was used as a reference. ΔCt represented the difference between Ct_{GAPDH} and $Ct_{target\ gene}$. The relative value of the target gene was computed with $2^{-\Delta Ct}$ because DNA doubled with 100% amplification efficiency in every cycle.

2.2.4 Enzyme-Linked ImmunoSorbent Assay (ELISA)

The ELISA was conducted according to the manufacturer's protocol. To begin with, all reagents, working standards, and samples were prepared and kept at RT before the experiment. 100μL of Assay Diluent RD1-56 was added to each well. After that, each well was added with 50μL of standard, control, or sample and covered with the adhesive strip. The plate was incubated for 2h at RT on a horizontal orbital microplate shaker set at 500rpm. Each well was aspirated and washed with 400μL wash buffer, and this process was repeated three times for a total of four washes. The plate was inverted and blotted against clean paper towels. After that, each well was added with 200μL of human thrombospondin-1 conjugate and covered with a new adhesive strip, followed by a 2h incubation at RT on the shaker. Then, the above aspiration/wash process was repeated, and 200μL of substrate solution was added to each well. The plate was subsequently incubated for 30min at RT in a dark room. 50 μL of stop solution was added to each well, and the color in the wells changed from blue to yellow. Finally, the optical density of each well was determined within 30min using a microplate reader

set at 450 nm, with the wavelength correction set at 540 nm. A standard curve was created using computer software, and the concentration of human THBS1 could be achieved then.

2.2.5 Wound Healing (WH) Test

For examination of PCCs migration, the standard protocol of WH assay was used. In brief, PCCs ($5x10^5$ cells/well) were seeded in 6-well plates in the incubator (37°C, 5% CO2/air, humid environment) until they reached 100% confluency. Cell monolayers were scratched with a tip (200μL) through every well. After being washed with PBS twice, PCCs were eliminated from cell fragments and were cultured under different conditions depending on the experiments. Images were captured at the time points of 0h and 24h at 100x magnification. The wound area was analyzed with ImageJ and used for further statistical analysis.

2.2.6 Transwell Migration and Invasion Assays

The migration and invasion abilities of PCCs were examined by performing experiments using transwell chambers coated with or without Matrigel.

Briefly, PCCs were cultivated using RPMI-1640 (1% FBS) for 24h. PCCs ($5x10^4$) were then suspended in 200μL FBS-free medium and added to the upper chamber, while 600μL medium with different conditions depending on the experiments was added to the bottom chamber as a chemoattractant. The PCCs were allowed to migrate or invade for 24h and 48h, respectively. After that, PCCs on the upper surface of the membrane were removed with cotton swabs. PCCs on the lower side were then stained with 0.1% crystal violet at RT for 20min. Migratory and invasive cells were counted in five representative microscopy fields under a light microscope (magnification 200x).

2.2.7 Western Blot

2.2.7.1 Protein extraction

To begin with, tissues were removed of adipose or connective parts, washed by PBS, and put into tubes. The tubes were then added with ice-cold lysis buffer rapidly, homogenized with a homogenizer, and maintained constant agitation for 2h at 4°C. Following centrifugation (20min, 12000rpm, 4°C), the tubes were placed on ice, and the supernatant was collected in new tubes and kept on ice.

2.2.7.2 Protein quantitation

The protein quantitation was conducted using the BCA Protein Assay Kit. According to the manufacturer's procedure, each well was filled with a 200μl reagent mixture (reagent A: B=50:1) and standard or target proteins (25μl). Afterward, the plate was maintained constant agitation for 30s at RT. After a 30min incubation at 37°C, the absorbance of the plate was measured at 562nm using a plate reader. The standard curve was achieved by plotting the relationship between the blank-adjusted average reading and the concentration (μg/mL).

2.2.7.3 Western blotting

2.2.7.3.1 Preparation of polyacrylamide gel

Ethanol and DIW were used to clean the glass sheets and spacers. Clean glass plates and spacers were then assembled on a flat and horizontal platform. The glass plates with spacers were added with a 10mL resolving gel solution (Table 2). Isopropanol was overlaid above the resolving gel (20-30min, RT) to keep a horizontal surface. After the removal of isopropanol, the stacking gel solution (Table 2) was added until it overflowed. A comb was immediately inserted, and any air bubbles between the gel and comb were

driven away manually. The gel was then left for 30min at RT for setting.

2.2.7.3.2 Polyacrylamide gel electrophoresis (PAGE)

Samples (containing equal volumes of proteins) and a weighted marker were gently added into SDS-PAGE wells. Running buffer (1x, Table 2) was poured into the electrophoresis apparatus. Afterward, the gel was run according to the manufacturer's protocol (100V, 1h).

2.2.7.3.3 Membrane transfer

PVDF membrane was activated with methanol for 25s. The membrane was then put into the transfer buffer before use (1x, Table 2). A rounded tweezer was used to deal with the membrane carefully to prevent scratches. Before the creation of the "transfer sandwich," filter papers and sponges were soaked in transfer buffer. After electrophoresis, the gel was isolated for the preparation of the sandwich. The sandwich layers were sequentially assembled, and any air bubbles should be removed gently with a tweezer as they could interfere with the transfer procedure. Finally, the sandwich was set in transfer equipment, and the wet transfer was performed according to the protocol.

2.2.7.3.4 Immunoblotting

After protein transfer, the membrane was washed with TBST (1x) solution 3 times. The membrane was then incubated overnight with blocking solution (Table 2) on a shaker (4˚C). Directed by the manufacturer's protocol, TBST (1x) solution containing 1% milk was used to make the primary Ab solution by diluting to working concentration. The membrane was then incubated in the primary Ab solution with gentle agitation (2h, RT). The membrane was washed three times and soaked into the secondary antibody

solution with gently shaking (1h, RT). After another three washes, the membrane was finally ready for further detection.

2.2.7.3.5 Detection

ECL substrate was made before use in accordance with the manufacturer's protocol. After a 3min incubation using ECL substrate, the membrane was exposed using a ChemiDoc MP imaging system (Bio-Rad). The grey values of the bands were measured by ImageJ software.

Table 2 The formulas of different solutions in WB

Solution	Chemicals	Doses
Resolving gel solution	30% Acr	3.4mL
	10% APS	100μL
	DIW	3.8mL
	10% SDS	100μL
	TEMED	10μL
	1.5M Tris-HCl (pH 8.8)	2.6mL
Stacking gel solution	30% Acr	1.34mL

	10% APS	100μL
	DIW	5.86mL
	10% SDS	100μL
	1.5M Tris-HCl (pH 6.8)	2.6mL
	TEMED	10μL
Running Buffer (10x)	DIW	1L
	Gly	144g
	SDS	10g
	Tris Base	30g
Running Buffer (1x)	DIW	900μL
	Running Buffer (10x)	100μL
Transfer Buffer (10x)	DIW	1L
	Gly	144g

	Tris Base	30g
Transfer Buffer (1x)	DIW	800mL
	Methanol	100mL
	Transfer Buffer (10x)	100mL
TBS (10x)	DIW	1L
	NaCl	80g
	PH	7.6
	Tris Base	24g
TBST (1x)	DIW	900mL
	TBS (10x)	100mL
	Tween 20	1mL
Protein lysis Buffer	Protease inhibitor	1 tablet
	RIPA buffer	100mL

Tris-HCl (1M) solution	DIW	200mL
	PH	6.8
	Tris-base	12.12g
Tris-HCl (1.5M) solution	DIW	200mL
	PH	8.8
	Tris-base	36.34g
Loading buffer	loading buffer (4x)	900μL
	β-Mercaptoethanol	100μL
SDS solution (10%)	DIW	100mL
	SDS	10g
APS solution (10%)	APS	10g
	DIW	100μL
Blocking solution	Milk powder	1g

TBST (1x)	20mL

2.2.8 EZ4U Assay

Cell proliferation was detected according to the manufacturer's protocol using an EZ4U kit. Briefly, cells ($1x10^4$ cells/well) were seeded in a 96-well plate utilizing 200μL RPMI-1640 medium (10% FBS) per well. After 24h, the culture medium was refreshed by new medium with different treatments according to the experiments. After 48h culture, 20μL dye substrate was added to every well and incubated for 3h. Finally, the absorbance of cells was determined using a microplate reader set at 450nm.

2.2.9 Bioinformatic Analysis

STRING database (https://string-db.org/) is a tool for analyzing the relationships (including physical and functional connections) between genes and establishing protein-protein interaction networks. Around 24 million proteins from 5,090 organisms were included in STRING (v11.0) [160]. In my project, papers on the differentially expressed genes in the activation procedure of PSCs were searched in PubMed. Then the protein-protein interaction networks among differentially expressed genes were analyzed using the STRING database.

GEPIA (http://gepia.cancer-pku.cn/index.html) is a web-based tool for analyzing the RNA sequencing expression data, and it provides functions involving differential gene expression analysis, correlation analysis, patient survival analysis, and so on. Data of the tumor and paired normal samples from The Cancer Genome Atlas (TCGA: http://portal.gdc.cancer.gov/) and the Genotype-Tissue Expression (GTEx: http://gtexportal.org/home/) databases were included [161]. In my study, THBS1 and CD47 mRNA expression in 33 different types of cancers (n=15204), including PDAC

(n=179) matched with paired normal tissues (n=171), was investigated using GEPIA. The survival analysis of PDAC patients on THBS1 and CD47 was also conducted with this online tool.

2.2.10 Statistical Analysis

Statistical analysis was conducted utilizing SPSS 21.0. The standard deviation of the mean (SD) meant the variance of mean values. Student t-test was applied for comparisons between two groups. All results, if appropriate, in this project were described as the mean ± SD. Each experiment was performed at least three times in triplicates. P-value (<0.05) was considered statistically significant.

3. Results

3.1 Prediction of THBS1 as a potential molecule regulated by VDR

VDR activation by its ligand normalized PSCs, thereby decreasing PSCs-augmented malignancy of PCCs in co-culture. To investigate the downstream molecules which might function in this PSCs-PCCs crosstalk, I searched for related publications in PubMed and made a prediction via the STRING database (as shown in Materials & Methods). Two papers on the analysis of the differential gene expression in the activation procedure of PSCs were found [122, 162]. These genes were then employed to generate an evidence-based protein-interaction network in STRING, demonstrating the connections between several molecules with VDR in PSCs. By the prediction, THBS1, IL6, TGF-β1 were the candidates that might interact with VDR (Figure 4). IL6 and TGF-β1 have been well investigated in the PSCs-PCCs crosstalk [94, 122, 163-165]. Since THBS1 is an ECM protein widely expressed in tumor stroma and correlated with the aggressiveness of several other cancers [166-170], my study will further explore the role of this protein in PDAC.

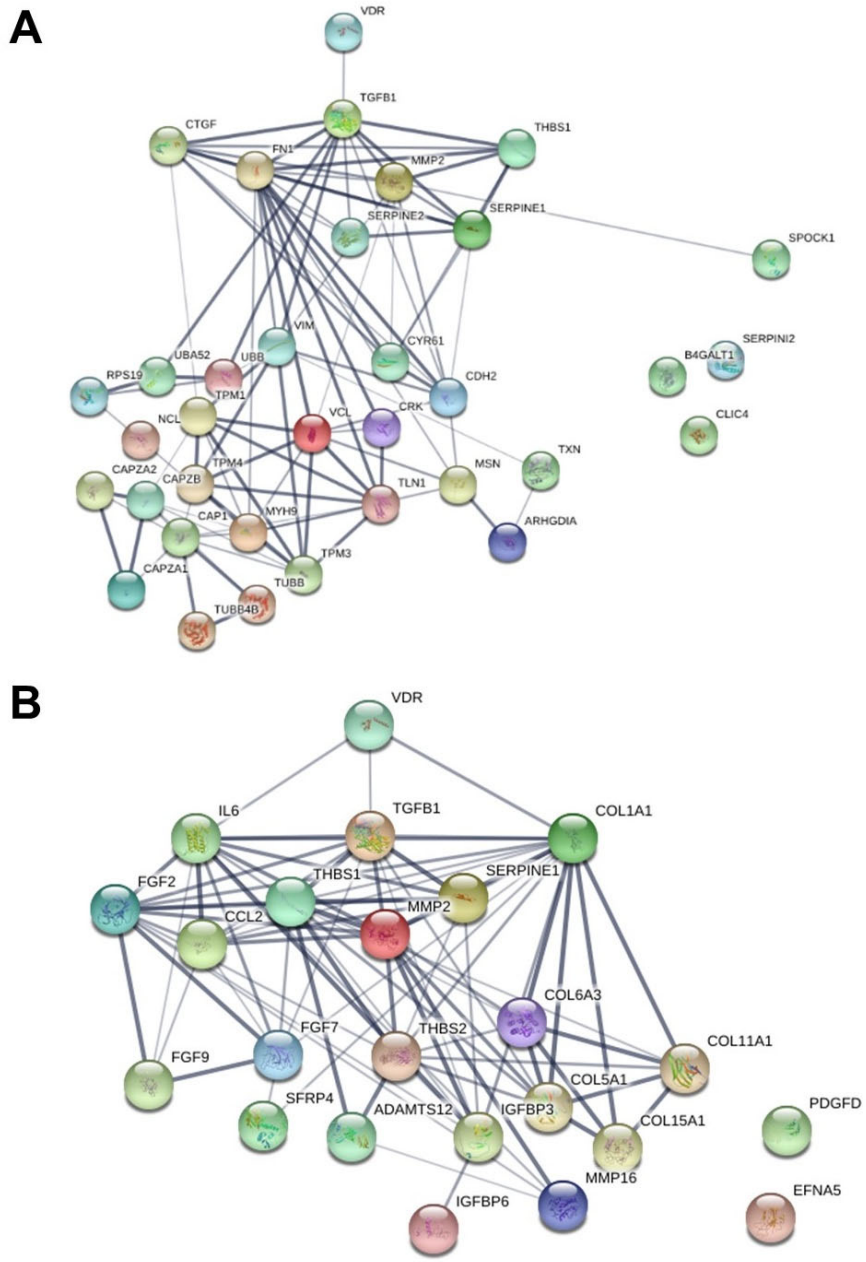

Figure 4: THBS1 was predicted as the potential protein interacting with VDR. Potential genes from Wehr et al. [162] (A) and Sherman et al. [122] (B) were employed to generate an evidence-based protein-interaction network in the STRING database, showing connections between several molecules with VDR in PSCs (Line thickness indicated the strength of data support).

3.2 THBS1 and CD47 are overexpressed in PDAC and are correlated with poor survival

To get a better understanding of the roles of THBS1 and its receptor CD47 in PDAC, I made bioinformatic analyses (see Materials & Methods 2.2.9) of THBS1, and CD47 mRNA levels in 33 different types of cancers (n=15204), including PDAC (n=179), matched with paired normal tissues (n=171), with online server GEPIA which is based on the database of TCGA and GTEx [161].

Compared with the adjacent normal group, THBS1 mRNA was significantly upregulated in the PDAC tumor group (Figure 5A-B). In addition, similar results were observed in CD47 at the mRNA level (Figure 6A-B).

Furthermore, I studied the relationship between the clinical prognosis of PDAC patients and the mRNA expression levels of THBS1 and CD47. Results showed that mRNA expression of THBS1 or CD47 was negatively correlated with the disease-free survival of PDAC patients (p=0.036 and 0.018, respectively) (Figure 5C and 6C).

These results showed that THBS1 and CD47 were dysregulated in PDAC and closely correlated with prognosis. Given the high expression of THBS1 in the stroma of many cancer, THBS1/CD47 axis might also play an essential role in the stroma-tumor interaction in PDAC.

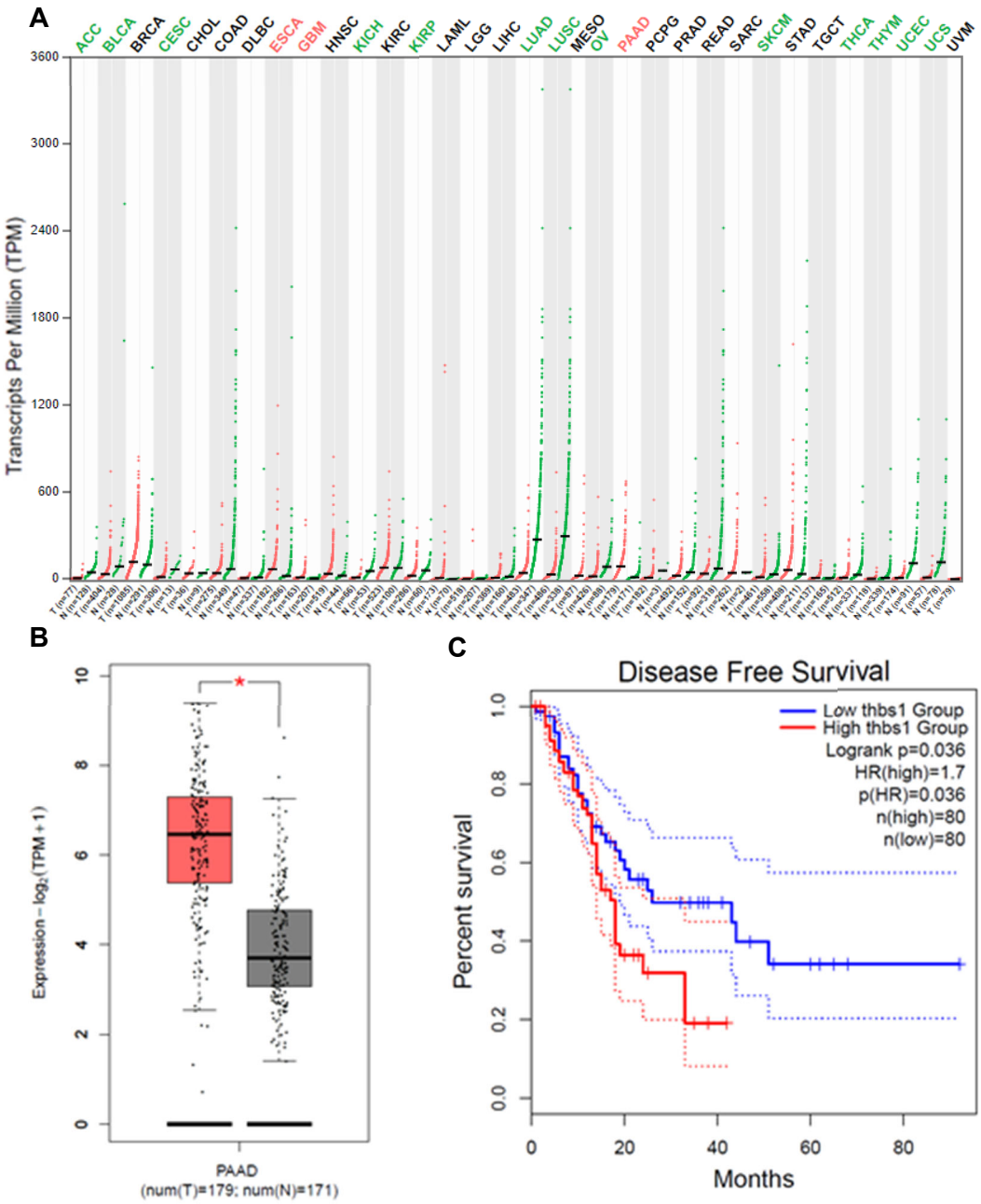

Figure 5: Expression of THBS1 was higher in PDAC and reduced survival. THBS1 mRNA level: (A) in paired normal-tumor tissue cohort in 33 cancers. (B) in PDAC (n=179) and paired normal tissues (n=171). *p<0.05. (C) Kaplan-Meier analysis indicating the relationship between THBS1 mRNA expression and disease-free survival of PDAC.

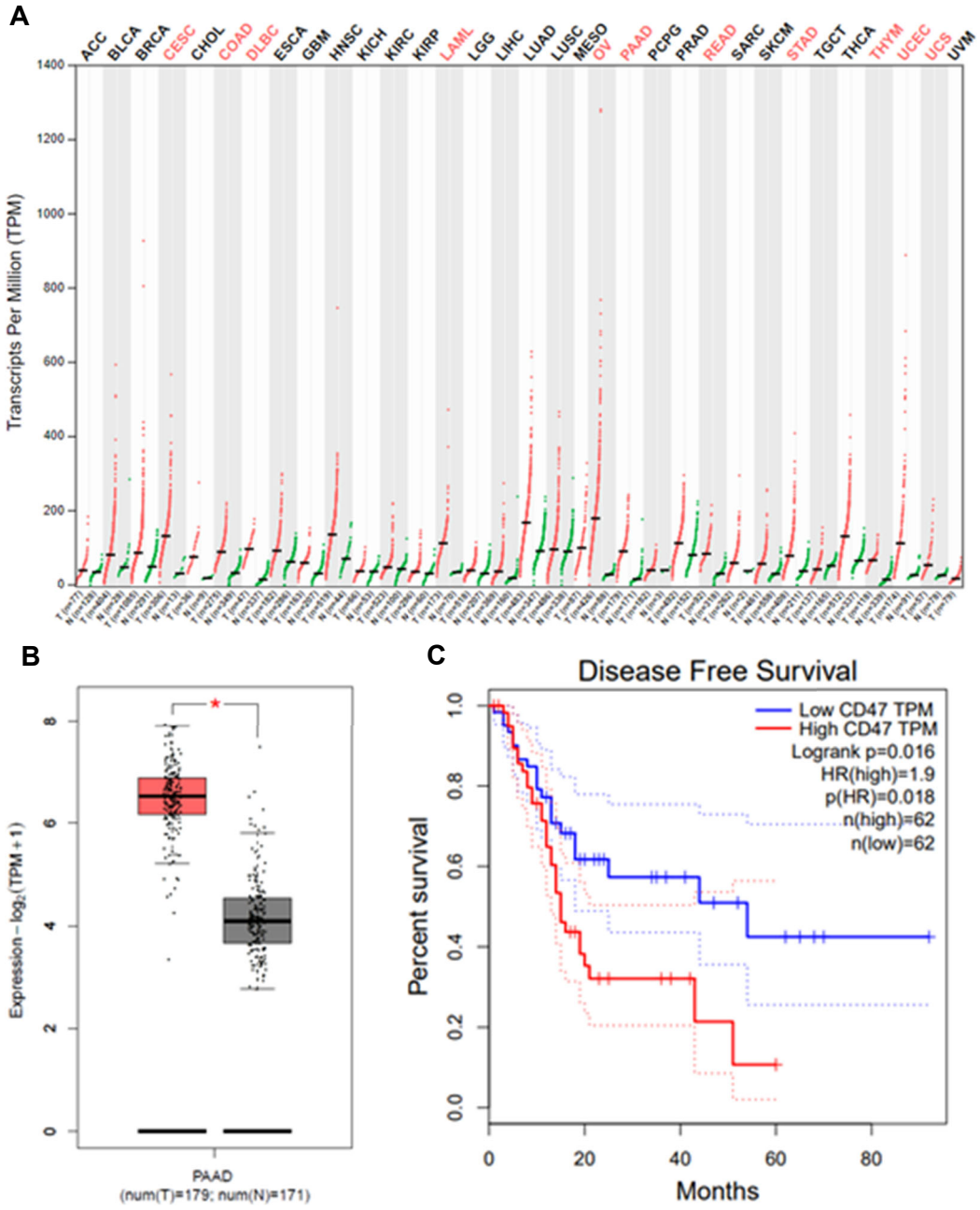

Figure 6: Expression of CD47 was higher in PDAC and reduced survival. CD47 mRNA level: (A) in paired normal-tumor tissue cohort in 33 cancers. (B) in PDAC (n=179) and paired normal tissues (n=171). *p<0.05. (C) Kaplan-Meier analysis indicating the relationship between CD47 mRNA expression and disease-free survival of PDAC.

3.3 CD47 protein is upregulated in PDAC

Then I performed a western blot analysis to investigate the protein expression of CD47 in PDAC. The result showed that the CD47 protein level was significantly higher in the tumor area of PDAC compared to the adjacent normal part (p=0.0222) (Figure 7). This further supported the results of the bioinformatic analysis above and indicated that CD47 could be an important receptor in PDAC development.

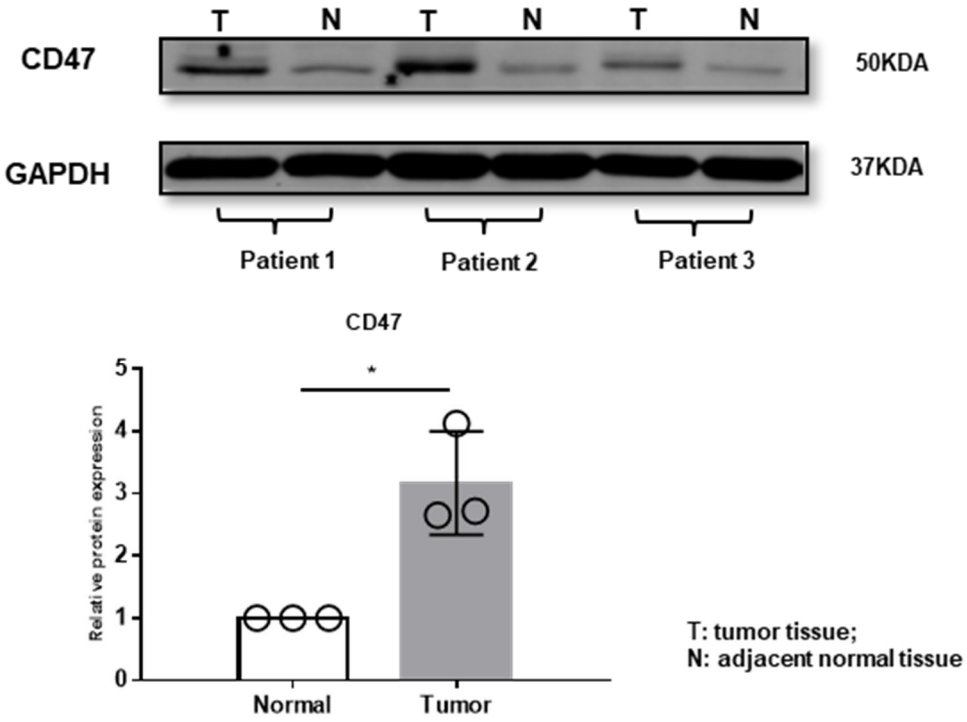

Figure 7: CD47 protein expression in PDAC was higher than adjacent normal area. Western Blot analysis showed CD47 protein level was significantly higher in tumor part of PDAC than adjacent normal part (p=0.0222). GAPDH was utilized as the loading control. Quantification determination was conducted by ImageJ. *p<0.05, **p<0.01, ***p<0.001, ****p<0.0001

3.4 PSCs secret higher THBS1 than PCCs

As reported in several cancers, THBS1 secretion rates by cancer-associated fibroblasts were at least one to two orders of magnitude higher than those by cancer cells [171-175]. However, no research was found on the THBS1 secretion by PSCs. Here, I detected THBS1 secretion in three different types of PSCs as well as three PDAC cell lines using ELISA. Results showed that all the three kinds of PSCs secreted significantly higher THBS1 than PCCs (p=0.0000, 0.0003, 0.0000), and the highest THBS1 secretion was observed in PSCs derived from the tumor (Figure 8).

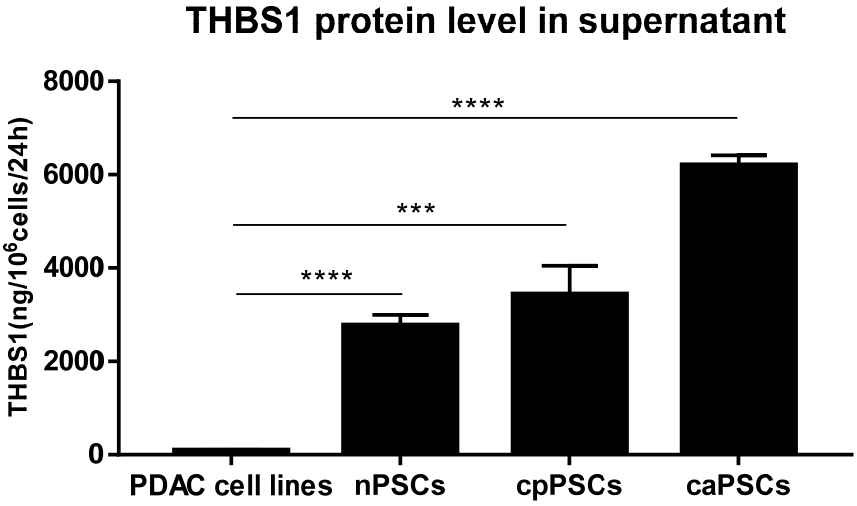

Figure 8: THBS1 secretion was higher in PSCs than PCCs. ELISA showed that PSCs, especially those derived from tumor, secreted higher THBS1 than PDAC cell lines (MIA PaCa-2, PANC-1, AsPC-1). nPSCs: normal PSCs; cpPSCs: PSCs from chronic pancreatitis; caPSCs: PSCs from PDAC. *p<0.05, **p<0.01, ***p<0.001, ****p<0.0001

3.5 The VD analog Cal decreases THBS1 secretion in PSCs

Next, I examined the effect of a VD analog, Cal, on THBS1 secretion in PSCs using ELISA. The results showed that after being treated with 100nM Cal for 48h, THBS1 protein levels in the supernatant of PSCs were significantly decreased compared to the control group (p=0.0000, 0.0018, 0.0026, respectively, Figure 9). This indicated that VDR induction by its ligand in PSCs could reduce the production of THBS1. This further demonstrated that THBS1 might be a critical molecular regulated by VDR and influence the PSCs-PCCs crosstalk.

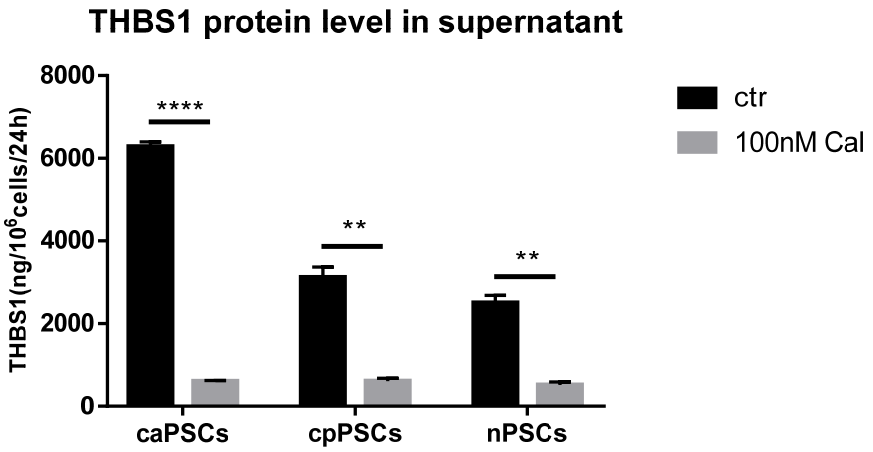

Figure 9: Cal decreased the THBS1 secretion in PSCs. ELISA was applied to test the change of THBS1 protein levels in the supernatant of PSCs from different origins after Cal treatment (100nM, 48h). VD analog was shown to decrease THBS1 secretion in all types of PSCs (n=3). *p<0.05, **p<0.01, ***p<0.001, ****p<0.0001

3.6 The VD analog Cal diminishes PSCs-augmented PCCs proliferation, invasion, migration, and EMT by downregulating THBS1/CD47 axis

As the results are shown above, PSCs secreted high THBS1, which could be inhibited by Cal. In addition, many studies have well proved that THBS1 can enhance the aggressiveness of several cancers [166-168, 176, 177]. Furthermore, our previous work indicated that the PSCs-augmented aggressiveness of PCCs in co-culture could be prevented by treating PSCs with Cal. Therefore, I proposed a hypothesis that Cal might downregulate PSCs-derived THBS1, thereby decreasing PCCs aggressiveness, and CD47 might mediate this process on PCCs. Here I further explored the role of the THBS1/CD47 axis in the PSCs-PCCs crosstalk.

3.6.1 Recombinant THBS1 (rTHBS1) increases the proliferation, migration, invasion, and EMT morphology of PCCs

Firstly, I investigated the effect of rTHBS1 on the proliferation ability of PCCs by EZ4U assay. Here I treated PCCs with different concentrations of rTHBS1 (0, 0.5, 5, 20μg/mL) and found that the proliferation abilities of both PANC-1 and MIA PaCa-2 were enhanced at 0.5μg/mL ($p=0.0349$, 0.0102 respectively), 5μg/mL ($p=0.0053$, 0.0006 respectively) and 20μg/mL ($p=0.0032$, 0.0015 respectively). The results showed that rTHBS1 treatment significantly enhanced proliferation abilities of both PANC-1 and MIA PaCa-2 in a dose-dependent manner (Figure 10).

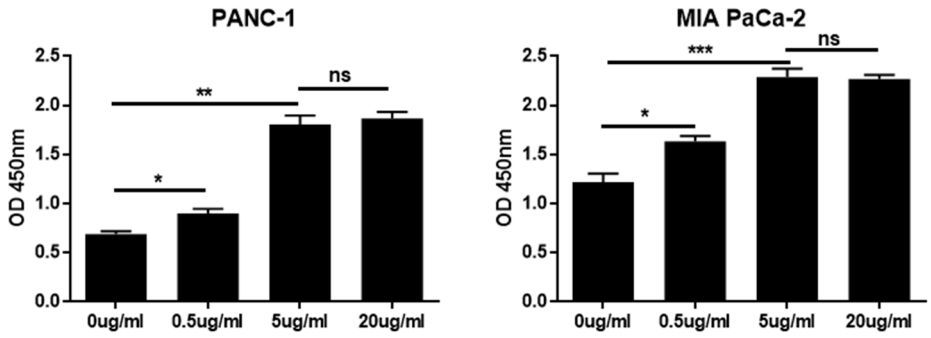

Figure 10: rTHBS1 increased PCCs proliferation in a dose-dependent manner. After rTHBS1 treatment, the proliferation of both PANC-1 (left) and MIA PaCa-2 (right) was enhanced at 0.5μg/mL, 5μg/mL, and 20μg/mL compared to the control group. *p<0.05, **p<0.01, ***p<0.001, ****p<0.0001

Then I explored the impact of rTHBS1 on the migration ability of PCCs via transwell migration assay and WH test. The results of the transwell migration assay showed that the treatment with rTHBS1 significantly increased the migration abilities of PANC-1 and MIA PaCa-2, both at 0.5 μg/mL (p=0.0125, 0.0083 respectively) and 5μg/mL (p=0.0000, 0.0000 respectively) (Figure 11).

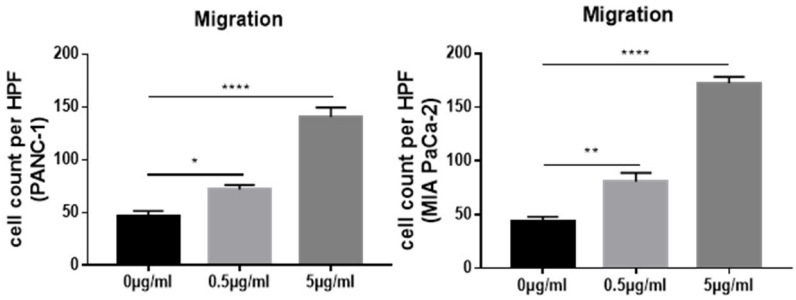

Figure 11: rTHBS1 increased PCCs migration in a dose-dependent manner (transwell migration assay). Quantification analysis of transwell migration assay displayed the effect of rTHBS1 on the migration capabilities of PANC-1 (left) and MIA PaCa-2 (right). *p<0.05, **p<0.01, ***p<0.001, ****p<0.0001

I further conducted the WH test to confirm the effect of rTHBS1 on PCCs migration and found similar results. WH test showed that the migration rates of both PANC-1 and MIA PaCa-2 were significantly enhanced by the treatment of rTHBS1 at 0.5μg/mL (p= 0.0162, 0.0083 respectively) and 5μg/mL (p=0.0033, 0.0005 respectively) (Figure 12). This result further confirmed that rTHBS1 treatment could enhance the migration abilities of PCCs in a dose-dependent manner.

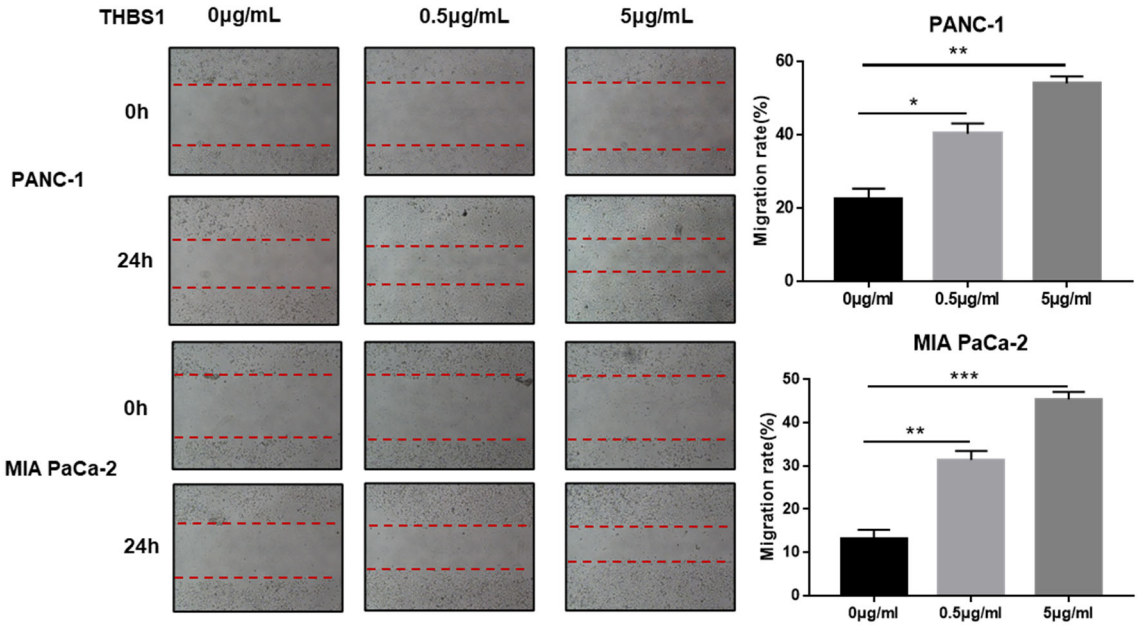

Figure 12: rTHBS1 increased PCCs migration in a dose-dependent manner (WH test). Representative images (left) and quantification analysis (right) of WH test displayed the effect of rTHBS1 on the migration capabilities of PANC-1 and MIA PaCa-2. *p<0.05, **p<0.01, ***p<0.001, ****p<0.0001

Furthermore, I investigate the effect of rTHBS1 on PCCs invasion by transwell invasion assay. The result showed that rTHBS1 significantly increased the invasion abilities of PANC-1 and MIA PaCa-2 both at 0.5 μg/mL (p=0.0299, 0.0157 respectively) and 5μg/mL (p=0.0040, 0.0010 respectively) (Figure 13).

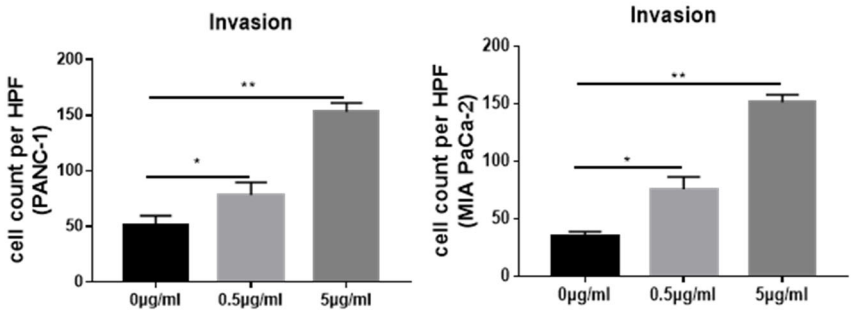

Figure 13: rTHBS1 increased PCCs invasion in a dose-dependent manner. Quantification analysis of transwell invasion assay exhibited the impact of rTHBS1 on the invasion abilities of PANC-1 (left) and MIA PaCa-2 (right). *p<0.05, **p<0.01, ***p<0.001, ****p<0.0001

As well proved by several studies, PSCs could induce EMT procedure of PCCs [163, 178-181]. Here I treated PCCs with PSCs-CM or rTHBS1. The result showed that after treatment with PSCs-CM or rTHBS1, PANC-1 and MIA PaCa-2 displayed typical morphological changes of EMT with a spindle-like shape with less cell-cell adhesion (Figure 14).

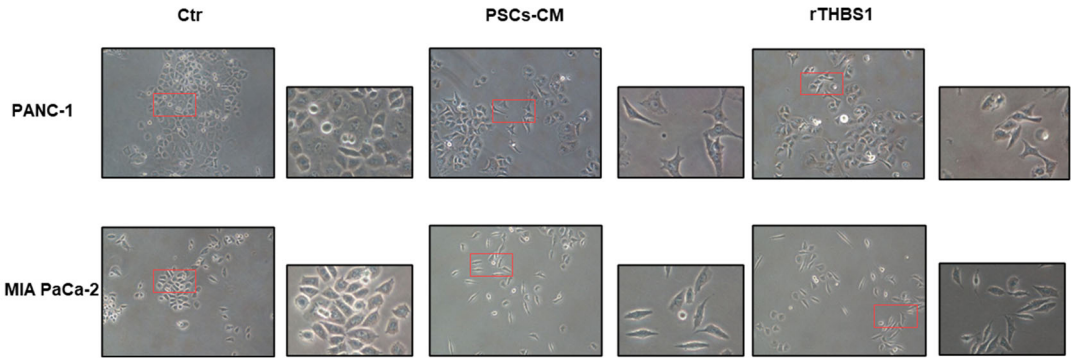

Figure 14: EMT morphological changes of PCCs after PSCs-CM or rTHBS1 treatment. After being treated by PSCs-CM or rTHBS1, PANC-1 and MIA PaCa-2 exhibited a spindle-like appearance with less cell-cell adhesion.

In conclusion, rTHBS1 increased the proliferation, migration, invasion abilities, as well as EMT morphology of PCCs.

3.6.2 THBS1 neutralizing Ab inhibits PSCs-CM-induced proliferation, migration, invasion, and EMT of PCCs

Furthermore, to determine whether Cal regulated the PSCs-induced aggressiveness of PCCs by modulating THBS1 expression, I used THBS1 neutralizing Ab to deplete THBS1 from CM of PSCs (PSCs-CM) or Cal-pretreated PSCs (Cal-PSCs-CM) and then cultured PCCs with the above CM. As shown in Figure 15, this treatment significantly decreased PSCs-CM-induced proliferation of PANC-1 and MIA PaCa-2 ($p=0.0133$, 0.0106 respectively) but did not affect Cal-PSCs-CM-induced PCCs proliferation ($p=0.3093$, 0.5727 respectively).

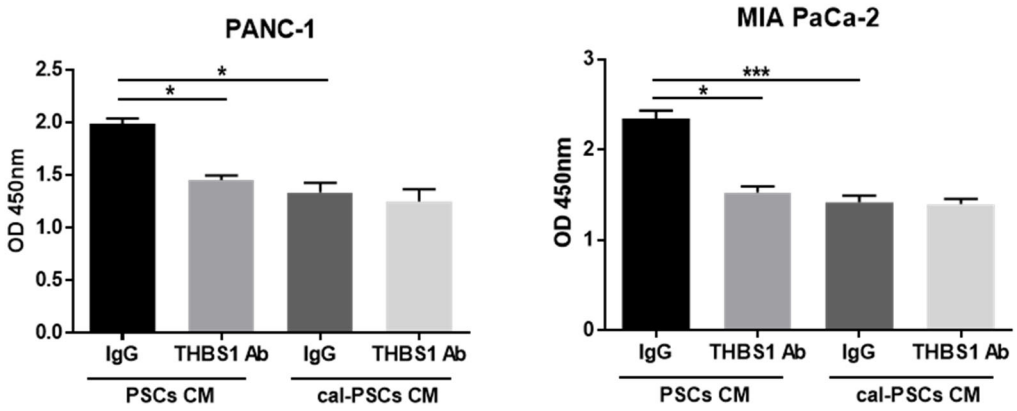

Figure 15: THBS1 neutralizing Ab inhibited PSCs-CM-induced PCCs proliferation. THBS1 neutralizing Ab significantly diminished PSC-CM-induced PCCs proliferation but not Cal-PSCs-CM-induced PCCs proliferation. CM from different PSCs was pretreated with 1μg/mL of THBS1

Ab or control IgG. *p<0.05, **p<0.01, ***p<0.001, ****p<0.0001

Then I conducted a transwell migration assay to confirm the THBS1 effect on the PSCs-induced migration ability of PCCs. The results showed that this treatment significantly diminished PSCs-CM-induced migration of PANC-1 and MIA PaCa-2 (p=0.0000, 0.0000 respectively) but had no effect on Cal-PSCs-CM-induced PCCs migration (p=0.1077, 0.8075 respectively) (Figure 16).

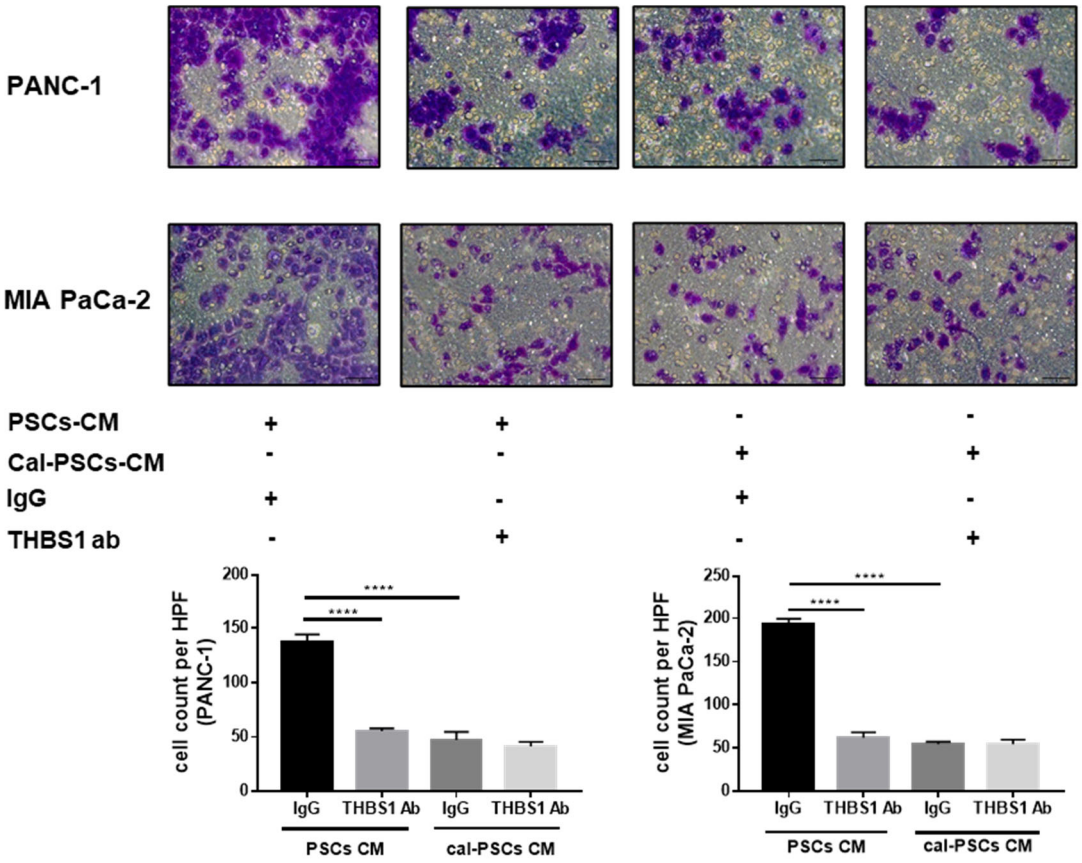

Figure 16: THBS1 neutralizing Ab inhibited the PSCs-CM-induced migration of PCCs (transwell migration assay). THBS1 neutralizing Ab significantly diminished PSCs-CM-induced cancer cell migration but not Cal-PSCs-CM-induced PCCs migration. CM was pretreated with 1μg/mL of THBS1 Ab or control IgG and then added into the lower chambers.

*p<0.05, **p<0.01, ***p<0.001, ****p<0.0001

Furthermore, I performed the WH test to confirm the effect of THBS1 Ab on PSCs-induced PCCs migration. The result showed that this treatment significantly decreased PSCs-CM-induced PCCs migration of PANC-1 and MIA PaCa-2 (p=0.0077, 0.0087 respectively) but had no effect on Cal-PSCs-CM-induced PCCs migration (p=0.2624, 0.2281 respectively) (Figure 17).

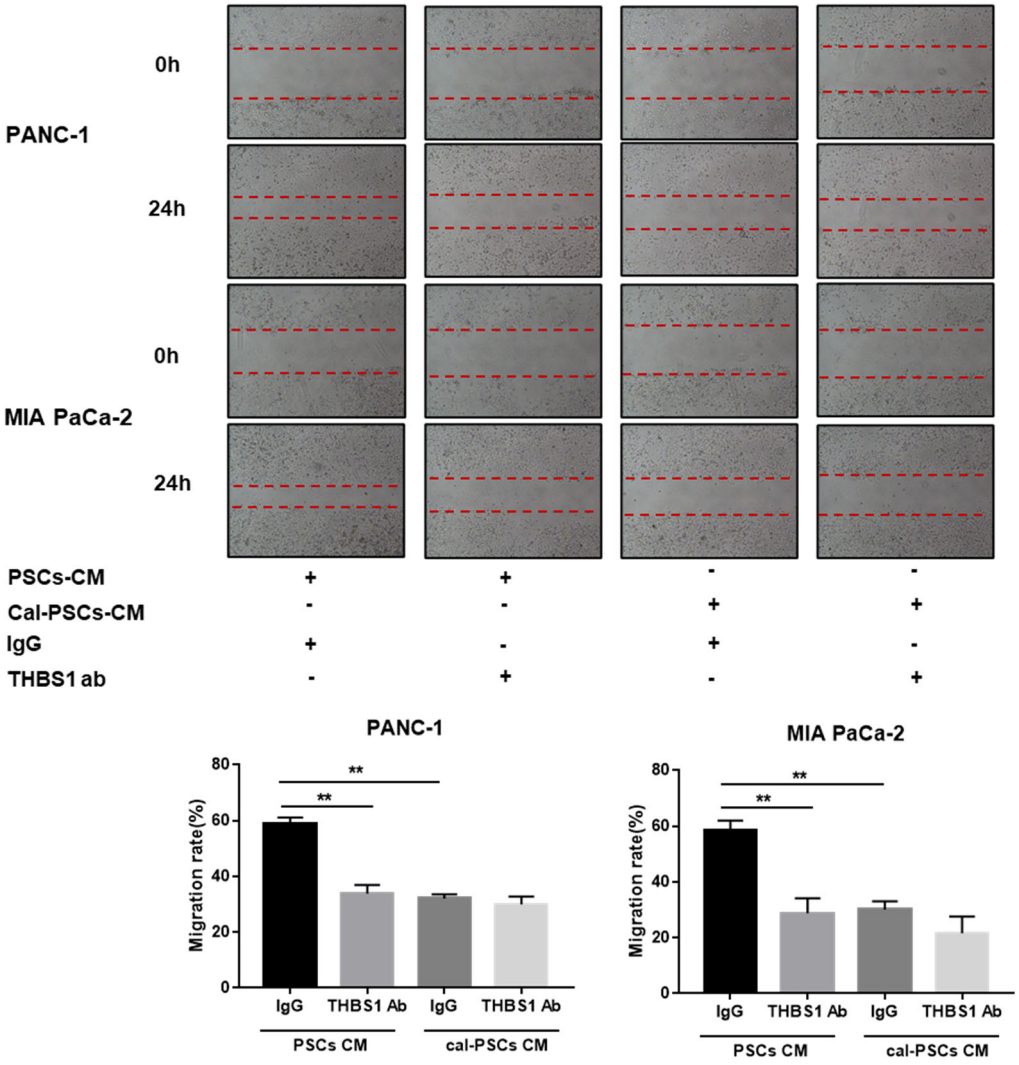

Figure 17: THBS1 neutralizing Ab inhibited the PSCs-CM-induced migration of PCCs (WH test). THBS1 neutralizing Ab significantly diminished PSCs-CM-induced PCCs migration but

not Cal-PSCs-CM-induced PCCs migration. CM was pretreated with 1μg/mL of THBS1 Ab or control IgG. *p<0.05, **p<0.01, ***p<0.001, ****p<0.0001

In addition, I conducted a transwell invasion assay to explore the effect of THBS1 Ab on PSCs-induced PCCs invasion abilities. As shown in Figure 18, THBS1 Ab decreased PSCs-CM-induced invasion of PANC-1 and MIA PaCa-2 (p=0.0000, 0.0000 respectively), while no impact was observed on Cal-PSCs-CM-induced PCCs invasion (p=0.3486, 0.2221 respectively).

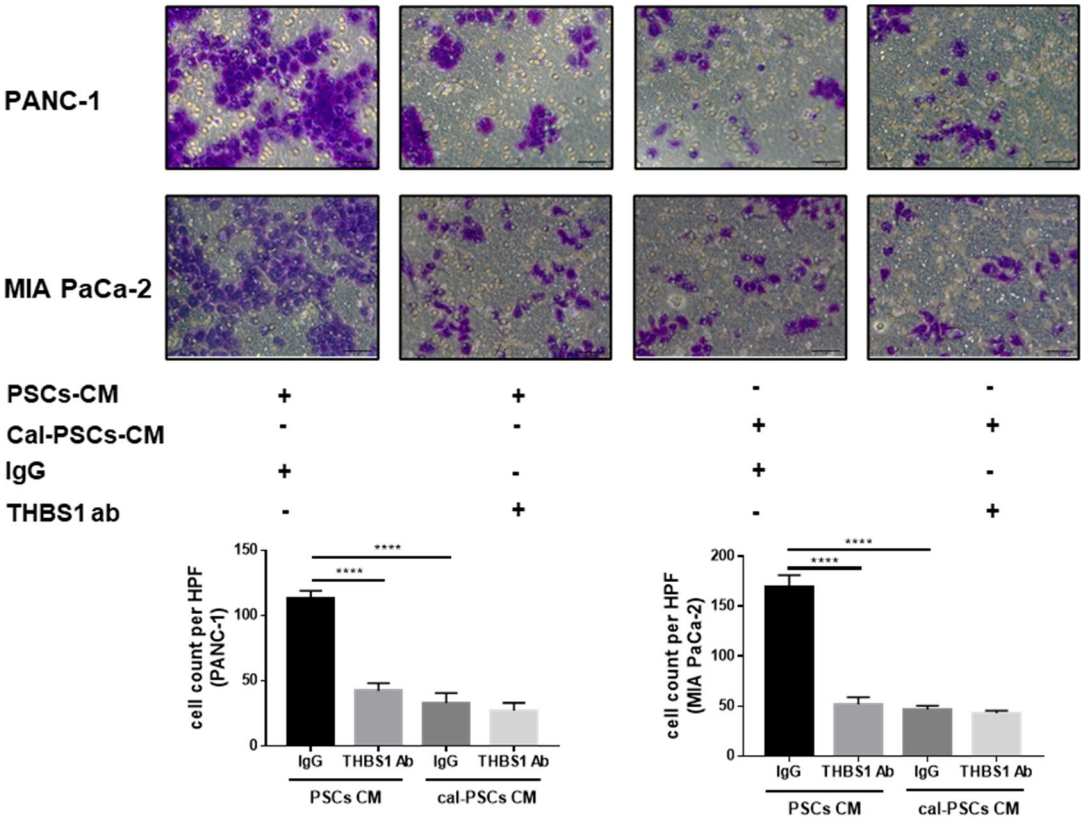

Figure 18: THBS1 neutralizing Ab inhibited the PSCs-CM-induced invasion of PCCs. THBS1 neutralizing Ab significantly diminished the PSCs-CM-augmented invasion of PCCs but not Cal-PSCs-CM-induced PCCs invasion. CM was pretreated with 1μg/mL of THBS1 Ab or

control IgG and then added into the lower chambers. *p<0.05, **p<0.01, ***p<0.001, ****p<0.0001

Finally, the EMT markers (E-cadherin, N-cadherin, Vimentin) were tested by qRT-PCR to explore the effect of THBS1 neutralizing Ab on PSCs-induced PCCs EMT. As shown in Figure 19, THBS1 Ab diminished PSCs-CM-induced EMT procedure in PCCs, while no impact was observed on Cal-PSCs-CM-induced PCCs. Specifically, the epithelial marker E-cadherin increased in PANC-1 and MIA PaCa-2 (p=0.0217, 0.0205 respectively), while the mesenchymal markers N-cadherin (p=0.0068, 0.0151 respectively) and Vimentin (p=0.0070, 0.0018 respectively) decreased.

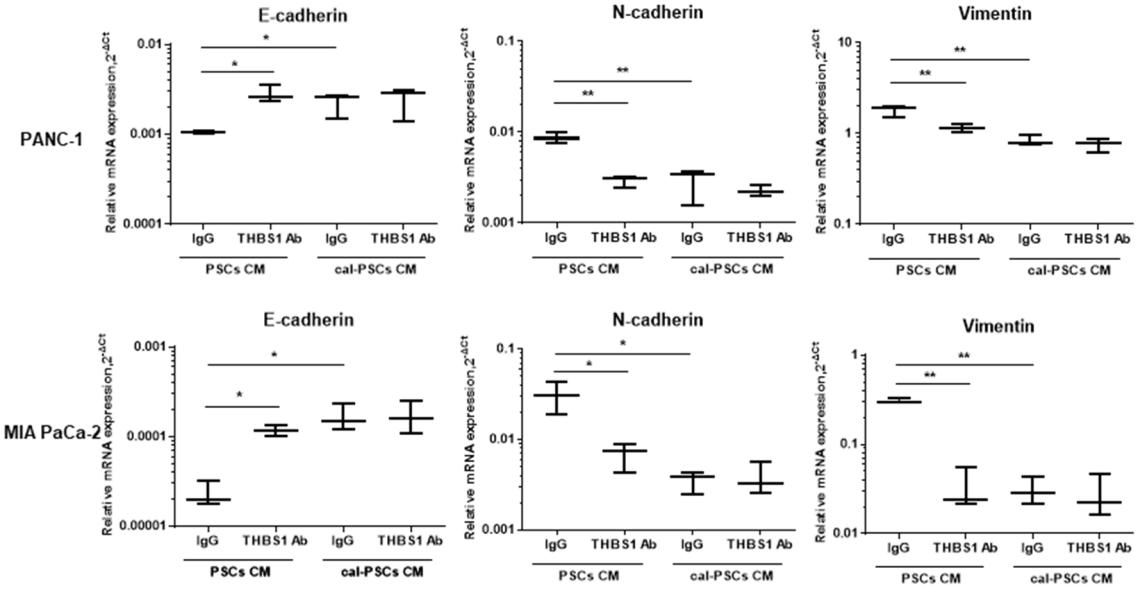

Figure 19: THBS1 neutralizing Ab inhibited the PSCs-CM-induced EMT procedure in PCCs. THBS1 neutralizing Ab significantly diminished the PSCs-CM-induced EMT procedure in PCCs but not the Cal-PSCs-CM-induced EMT in PCCs. *p<0.05, **p<0.01, ***p<0.001, ****p<0.0001

In summary, these findings indicated that Cal decreased PSCs-augmented proliferation, invasion, migration, and EMT of PCCs by downregulating THBS1.

3.6.3 CD47 blocking Ab inhibits PSCs-CM-induced proliferation, migration, invasion, and EMT of PCCs

Since THBS1 was reported to induce aggressiveness of tumor cells primarily by binding to CD47 in several cancers, I used a CD47 blocking Ab to investigate whether CD47 mediated the effect of THBS1 on PSCs-PCCs crosstalk or not.

Firstly, results from the EZ4U assay indicated that blocking CD47 in PCCs significantly inhibited PSCs-CM-induced proliferation of PANC-1 and MIA PaCa-2 (p=0.0094, 0.0019 respectively) but did not affect Cal-PSCs-CM-induced cell proliferation (p=0.5922, 0.4158 respectively) (Figure 20). These results showed that THBS1-induced proliferation of PCCs was mediated by CD47.

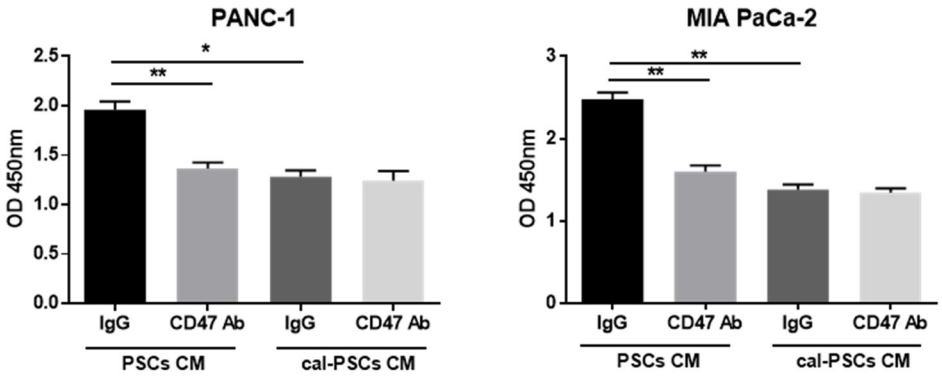

Figure 20: CD47 blocking Ab inhibited the PSCs-CM-induced proliferation of PCCs. CD47 blocking Ab significantly reduced PSCs-CM-induced proliferation of PCCs but not Cal-PSCs-CM-induced proliferation of PCCs. PCCs were pretreated with 2μg/mL of CD47 blocking Ab or control IgG. *p<0.05, **p<0.01, ***p<0.001, ****p<0.0001

Transwell migration assay showed that this treatment significantly reduced the PSCs-CM-induced migration of PANC-1 and MIA PaCa-2 (p=0.0002, 0.0000 respectively) but had no effect on the Cal-PSCs-CM-induced migration of PCCs (p=0.0814, 0.8624

respectively) (Figure 21).

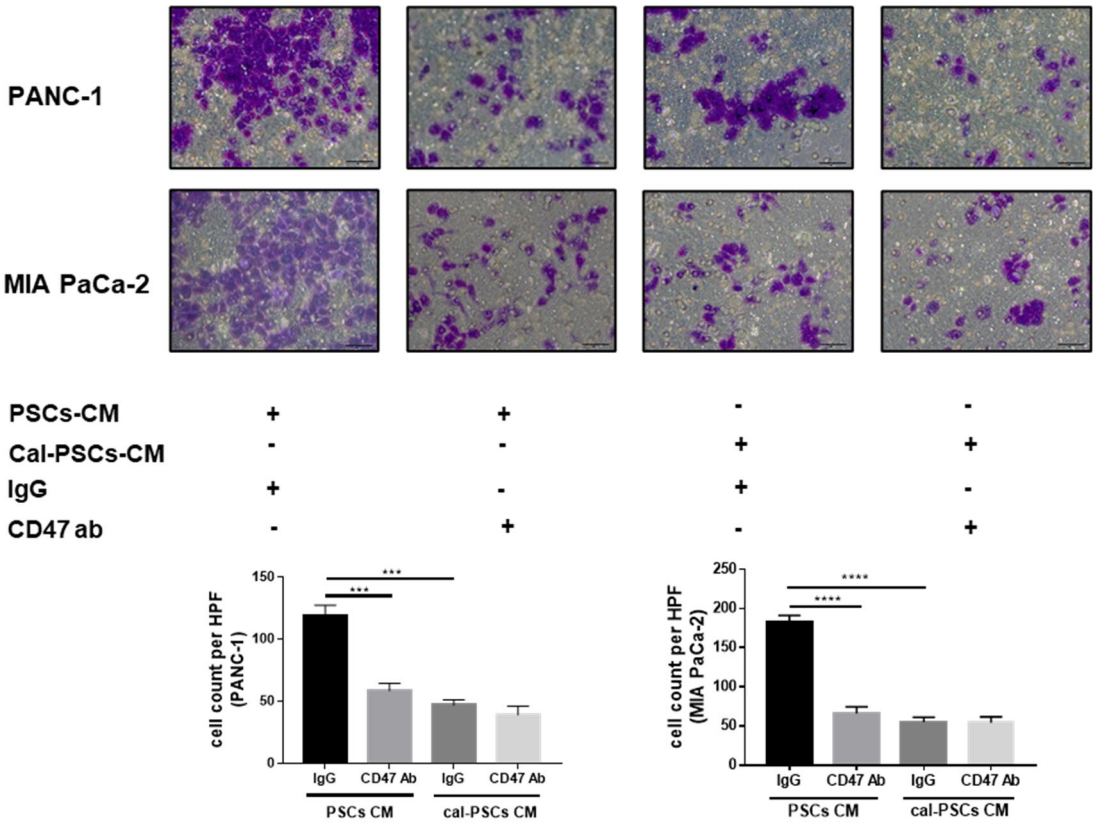

Figure 21: CD47 blocking Ab inhibited the PSCs-CM-induced migration of PCCs. CD47 blocking Ab significantly decreased the PSCs-CM-induced migration of PCCs but not the Cal-PSCs-CM-induced migration of PCCs. *p<0.05, **p<0.01, ***p<0.001, ****p<0.0001

Furthermore, I conducted the WH test to validate the impact of CD47 Ab on the PSCs-augmented migration of PCCs. The results also indicated that this treatment significantly diminished the PSCs-CM-induced migration of PANC-1 and MIA PaCa-2 (p=0.0017, 0.0101 respectively) but had no effect on the Cal-PSCs-CM-induced migration of PCCs (p=0.3599, 0.4326 respectively) (Figure 22).

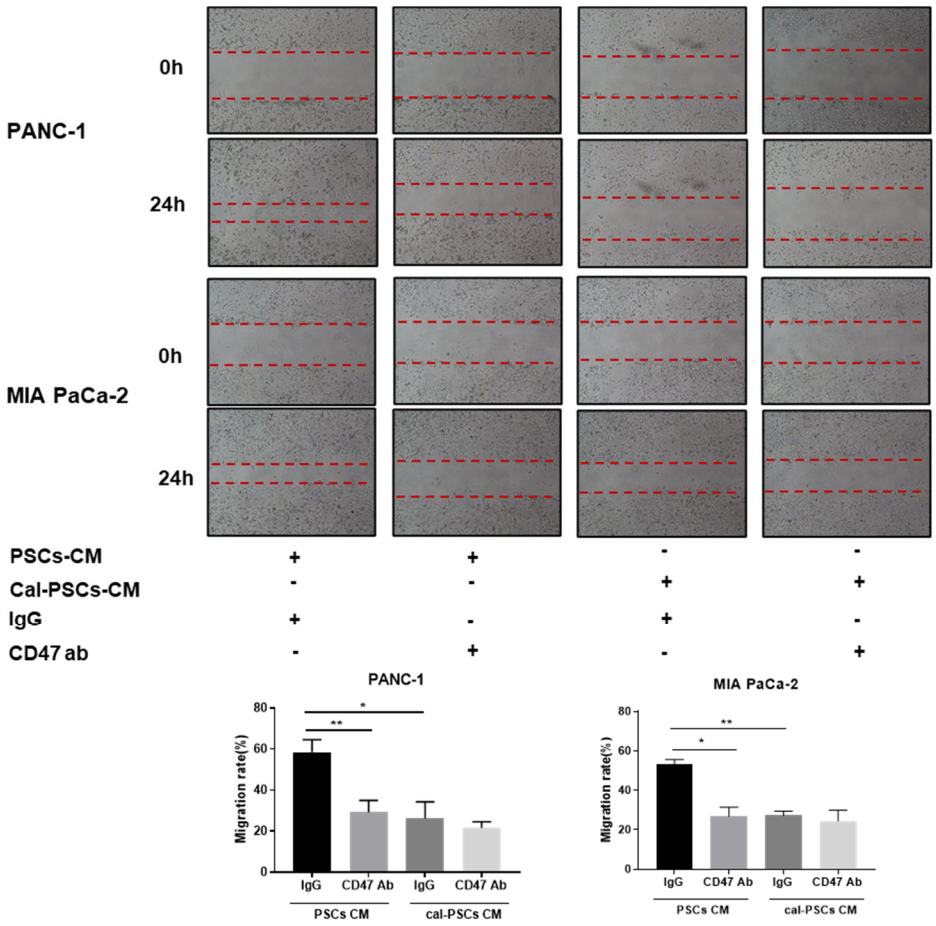

Figure 22: CD47 blocking Ab inhibited the PSCs-CM-induced migration of PCCs (WH test). CD47 blocking Ab significantly diminished the PSC-CM-induced migration of PCCs but not the Cal-PSCs-CM-induced migration of PCCs. *p<0.05, **p<0.01, ***p<0.001, ****p<0.0001

Additionally, I performed a transwell invasion assay to investigate the impact of CD47 Ab on PSCs-induced invasion abilities of PCCs. As exhibited in Figure 23, CD47 Ab diminished the PSCs-CM-induced invasion of PANC-1 and MIA PaCa-2 (p=0.0000, 0.0000 respectively), while no impact was observed on the Cal-PSCs-CM-induced invasion of PCCs (p=0.4977, 0.2005 respectively).

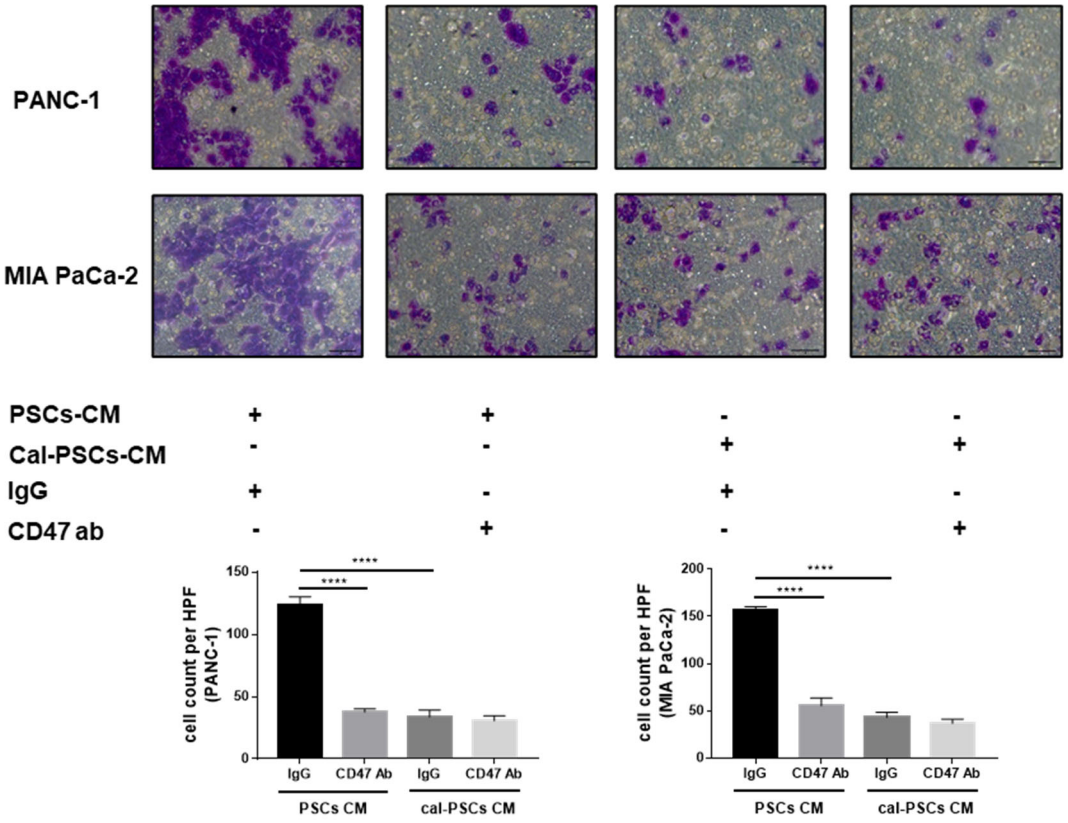

Figure 23: CD47 blocking Ab inhibited PSCs-CM-induced invasion of PCCs. CD47 blocking Ab significantly diminished the PSC-CM-induced invasion of PCCs but not the Cal-PSCs-CM-induced invasion of PCCs. *p<0.05, **p<0.01, ***p<0.001, ****p<0.0001

Lastly, the EMT markers (E-cadherin, N-cadherin, Vimentin) were detected by qRT-PCR to investigate the impact of CD47 blocking Ab on PSCs-augmented EMT procedure in PCCs. As exhibited in Figure 24, THBS1 Ab reduced PSCs-CM-induced EMT of PCCs, while no effect was observed on the Cal-PSCs-CM-induced EMT of PCCs. Specifically, the epithelial marker E-cadherin increased in PANC-1 and MIA PaCa-2 (p=0.0241, 0.0071 respectively), while the mesenchymal markers N-cadherin (p=0.0074, 0.0266 respectively) and Vimentin (p=0.0240, 0.0080 respectively) decreased.

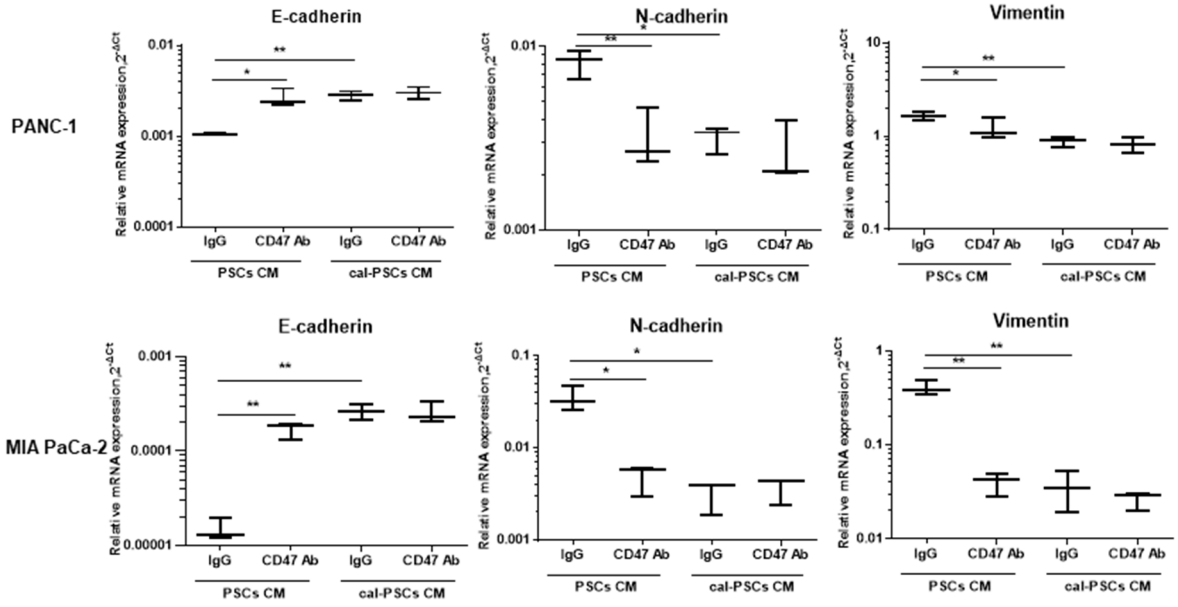

Figure 24: CD47 blocking Ab inhibited the PSCs-CM-induced EMT of PCCs. CD47 blocking Ab significantly diminished the PSCs-CM-induced EMT procedure of PCCs but not the Cal-PSCs-CM-induced EMT of PCCs. *p<0.05, **p<0.01, ***p<0.001, ****p<0.0001

These results indicated that CD47 was involved in the PSCs-PCCs crosstalk, and CD47 blockade could reduce PSCs-augmented proliferation, invasion, migration, and EMT of PCCs.

4. Discussion

4.1 VDR is a feasible target in PDAC treatment

Accumulating evidence has shown that the VDR system plays a vital role in cancer development, and VD analogs have been evaluated in many preclinical experiments and clinical trials to treat different cancers.

In our previous experiments conducted by Wu et al. [158], VDR expression of cancer-associated PSCs was significantly higher than that of pancreatic cancer cell lines, which was similar to the results of Sherman et al. [122]. This demonstrates that VDR is a druggable target of PSCs and is of high potential in developing PDAC therapy. In addition, our group previously showed that the VD analog Cal could significantly decrease αSMA expression (an activation marker of PSCs), migration, and proliferation of PSCs using WB, qRT-PCR, ICC, wound healing test, transwell assay, and EZ4U [158]. This indicated that Cal could attenuate the activation of PSCs. Consistent results were also found in the published paper, which showed that VD analogs could decrease PSCs activation (reduced αSMA mRNA expression and increased lipid droplets formation) [122].

Similarly, Wallbaum et al. indicated that VD analog decreased protein expression of αSMA and inhibited loss of lipid droplets in murine PSCs [182]. Kang et al. invented a novel VD analog which could reduce αSMA protein expression and ECM deposition, thereby inhibiting fibrosis in mouse pancreas with chronic pancreatitis [183]. Blauer et al. showed that $1,25(OH)_2D_3$ diminished proliferation and ECM production of murine PSCs [184]. Given the vital role of activated PSCs in the progression of PDAC, VDR is a promising target for the development of PSCs-targeted strategies.

It is well acknowledged that activated PSCs can enhance the malignancy of PCCs by various pathways. The strategy of simple depletion of PSCs has failed, which increased the malignancy of cancer cells, indicating the multifunctional role of PSCs in tumor development. Nowadays, reprogramming but not simply depleting PSCs has become a research hotspot. Therefore, many therapeutic strategies targeting PSCs for the treatment of PDAC have been proposed recently, such as vitamin A analogs, Ang-II inhibitors, SHH pathway inhibitors, and so on.

Since our group previously revealed the role of Cal in normalizing PSCs, I further investigated the effects of Cal on the PSCs-augmented aggressiveness of PCCs, including proliferation, migration, invasion, and EMT. In my study, PCCs cultured with the conditioned medium from Cal-pretreated PSCs showed a diminished proliferation, migration, invasion, and EMT compared to the control group. This further confirmed the hypothesis that the VD analog Cal might deactivate PSCs, thereby hindering the PSCs-induced aggressiveness of PCCs. In addition, a recent study showed that drug combination (Cal+GEM) could reduce the tumor volume and increase survival in the mouse model of PDAC, compared to GEM treatment alone. Therefore, repurposing VD analogs is feasible in enhancing the treatment of PDAC by reprogramming PSCs.

Several clinical trials are also found. A single application of VD analogs seems to be ineffective in the treatment of PDAC. Evans et al. indicated that EB1089 (a VD analog) had no anti-tumor effects on patients with inoperable PDAC [149]. Another VD analog, Arachitol, was evaluated by Barreto et al. in India. They demonstrated that intramuscular injection of Arachitol could not influence the overall morbidity and mortality rates of PDAC patients [150]. Nevertheless, drug combination with VD analogs and traditional chemotherapy drugs shows good prospects. Blanke et al. conducted a phase II trial to evaluate the drug combination (calcitriol+docetaxel) in 25 patients with unresectable PDAC [151]. Though side effects (e.g., hyperglycemia,

fatigue) were observed, patients treated with this drug combination exhibited an increase in time to progression compared to those only treated with docetaxel [151]. More recently, another drug combination (nivolumab, cisplatin, nab-paclitaxel, paricalcitol, GEM) was evaluated in a phase II study (NCT02754726). Preliminary data from 24 patients were encouraging, showing that the objective response rate was 83%, with a median PFS of 8.17 months and a median OS of 15.3 months [152]. Several other clinical trials (NCT03472833, NCT03331562, NCT03520790, NCT03300921, NCT03883919, NCT03519308, NCT03415854) investigating the combination treatment of VD analogs and chemotherapy drugs are underway.

Overall, targeting VDR is a promising therapeutic strategy to enhance conventional chemotherapy in PDAC as well as other stroma-rich tumors by remodeling stroma. It is also necessary to study the underlying mechanism (e.g., molecular pathways in the crosstalk), by which VD analogs reshape the PDAC microenvironment and inhibit the PSCs-PCCs interaction.

4.2 PSCs are vital sources of THBS1 in PDAC

Since PSCs have been well proved to release numerous factors which increase the aggressiveness of PCCs [72, 80, 94, 142, 185-189], targeting the paracrine interaction between PSCs and PCCs has become a research hotspot recently.

As VDR induction by its ligand has been shown to inhibit the PSCs-PCCs interaction, I further explored the molecules which might function in this procedure. By the STRING database analysis, I found that THBS1 might be a potential protein interacting with VDR and might play a role in the PSCs-enhanced malignancy of PCCs.

THBS1 is a 450-kDa ECM protein rich in stroma. It is the first identified member in the family of thrombospondins and is a critical player in TME where it induces an aggressive tumor behavior, especially through interaction with the CD47 receptor in several cancers [190].

Data of recent investigations have indicated that THBS1 was highly expressed in the stroma area of PDAC [191, 192]. Interestingly, several studies showed that THBS1 secretion rates by fibroblasts were significantly higher than those by tumor cells in different cancers [171-175]. Detailed information can be found in Table 3. Since PDAC-associated fibroblasts are mainly derived from PSCs, PSCs are mostly like the potential sources of THBS1 in PDAC.

For the first time, I used ELISA to test THBS1 secretion in PSCs with different origins (normal, CP, and PDAC) as well as three pancreatic cancer cell lines. The results indicated that all kinds of PSCs secreted much higher THBS1 than PCCs. It is worth noting that tumor-derived PSCs showed the most elevated secretion of THBS1 among all the PSCs with different origins. Therefore, my result indicated that PSCs were the primary producers of THBS1 in PDAC.

In addition, studies have shown that Vitamin D is closely related to THBS1. Adegoke et al. revealed an inverse relationship between serum 25-hydroxyvitamin D and THBS1 in children with vaso-occlusive crisis [193]. Vitamin D supplementation was shown to markedly decrease THBS1 levels and blood pressure in healthy individuals [194]. In atherothrombosis research, Vitamin D analogs paricalcitol and calcitriol could downregulate mRNA and protein expression of THBS1 [195, 196]. Quiroz et al. indicated that Calcitriol could reduce THBS1 secretion in breast cancer cells[197]. However, few studies were found in PDAC research. In the current study, I treated different types of PSCs with Cal and found that this VD analog could significantly decrease the THBS1 secretion in PSCs.

In summary, my results revealed that PSCs were essential sources of THBS1 secretion, and the VD analog Cal was able to reduce PSCs-derived THBS1. Given that THBS1 has been proved to increase aggression in several cancers, the extremely high release of THBS1 by PSCs might partly explain the PSCs-induced pro-tumorigenic ability in PDAC.

Table 3 THBS1 secretion by human cancer cells and fibroblasts

Cell types	THBS1 secretion (ng/10^6 cells/24h) [reference]
PDAC (AsPC-1, Colo-357, PANC-1, T3M4)	276; 61; 90; 94 [171]
PDAC (AsPC-1, PANC-1, Mia PaCa-2)	103, 81, 78 (current study)
Breast carcinoma (YMB-1)	3 [172]
Lung carcinoma (A549)	20 [172]
Gastric carcinoma (NUGC-4)	31 [172]
Liver carcinoma (HLF)	89 [172]
Colon carcinoma (Colo-201)	3 [172]
Prostate carcinoma (PC3)	610 [172]

Melanoma (DFB)	8 [172]
Neuroblastoma (IMR-32)	4 [172]
B-Chronic lymphocytic leukemia	9 [173]
Foreskin fibroblast	474 [171]; 15700 [174]; 3333 [175]
Fetal lung fibroblast	5800 [174]
PSCs from normal pancreas	2771 (current study)
PSCs from chronic pancreatitis	3438 (current study)
PSCs from pancreatic cancer	6203 (current study)

4.3 THBS1 and CD47 are involved in the progression of PDAC

Recent studies have shown that THBS1 plays an important role in cancer metastasis and aggressiveness. Pal et al. found that THBS1 increased the migration and invasion abilities of oral squamous cell carcinoma cells (OSCC) and induced the secretion of MMPs, thereby enhancing the malignancy of OSCC [198]. Borsotti et al. showed that THBS1 expression was higher in primary and metastases melanomas [170]. In another study, THBS1 promoted an aggressive behavior of tumor cells by inducing EMT in human melanoma [169]. Horiguchi et al. indicated that the expression of THBS1 was high in stromal components of invasive breast cancer and was positively correlated with enhanced lymph node metastasis [168]. In prostate cancer, high THBS1 expression was found to be significantly associated with invasive tumors and tumor recurrence [167]. Huang et al. found that FGF7/FGFR2 could upregulate THBS1, thereby increasing the invasion and migration of gastric cancer [199]. An in-vivo study by Yee et al. indicated that THBS1 in TME enhanced lung metastasis in the transgenic mouse model of breast cancer [166]. Daubon et al. demonstrated that THBS1 increased invasion via its receptor CD47 in tumor cells in glioblastoma [200]. Jeanne et al. utilized TAX2 to block the interaction between THBS1 and CD47, which inhibited metastasis and growth of melanoma cells in human malignant melanoma xenografts [201].

In the field of pancreatic cancer, research on the THBS1/CD47 axis is still lacking. Okada et al. revealed that high stromal THBS1 expression was correlated with poor prognosis and invasiveness in intraductal papillary-mucinous neoplasm (the precursor lesions of PDAC) of the pancreas [202]. This indicated that THBS1 might play a significant role even in the initial stage of PDAC. With the online server GEPIA, I made the bioinformatic analyses and found that THBS1 and CD47 mRNA expression were significantly higher in PDAC tumor tissue than those in paired normal tissue. In

addition, higher expression of THBS1 and CD47 was correlated with shorter disease-free survival. Therefore, the THBS1/CD47 axis is most likely to participate in the progression of PDAC and deserves further study.

Existing literature showed that THBS1 could enhance the invasion of PCCs in vitro [171, 203]. I performed a more detailed and comprehensive study to explore the effects of THBS1 on the aggressiveness of PCCs. In my research, recombinant THBS1 was shown to induce proliferation, migration, invasion, and EMT morphology changes of PCCs. This indicated that THBS1 was a key player in the tumor progression of PDAC. Combining my previous results that Cal could reduce the THBS1 secretion in PSCs, the ability of Cal to prevent PSCs-augmented malignancy of PCCs is probably mediated by downregulating PSCs-derived THBS1.

However, no published studies thoroughly investigating the role of VDR/THBS1/CD47 were found in PDAC research. Therefore, I used THBS1 neutralizing antibody and CD47 blocking antibody to explore further the role of THBS1/CD47 axis in PSCs-augmented aggressiveness of PCCs. The outcomes showed that both THBS1 neutralizing Ab and CD47 blocking Ab inhibited the PSCs-induced aggressiveness (proliferation, migration, invasion, EMT) of PCCs. This further confirmed the pro-tumorigenic role of the THBS1/CD47 axis in PDAC. In addition, these effects were not observed in PCCs cultured with CM from Cal-deactivated PSCs, further indicating that Cal could downregulate the THBS1/CD47 axis in the PSCs-PCCs crosstalk.

Combining the previous and current results of our group, I verified the hypothesis that the VD analog Cal could significantly reduce the activation, proliferation, migration of PSCs. The deactivated PSCs reduced the release of THBS1, thereby diminishing the PSCs-augmented cancer aggressiveness via its receptor CD47 on PCCs.

4.4 The THBS1/CD47 axis is a promising target in PDAC treatment

Since my results have indicated the critical role of the THBS1/CD47 axis in PDAC progression, targeting this axis is promising in developing an effective therapy for PDAC.

Several studies have suggested the strategy of THBS1 depletion. Leca et al. found that depletion of THBS1-containing extracellular vesicles in CAFs reduced tumor growth and metastasis in PDAC mouse models [191]. Jeane et al. revealed that blockade of THBS1 with a newly designed peptide significantly inhibited the growth rate and vascularization of PDAC xenografts in nude mice [204]. In my study, depletion of PSCs-derived THBS1 markedly reduced the aggressiveness of PCCs in vitro. All these suggest that THBS1 is a key player in stroma-tumor interaction and targeting THBS1 is feasible in the development of PDAC therapy.

The CD47 blockade strategy for PDAC has also been reported recently. Pan et al. revealed that CD47 blockade with a monoclonal antibody reduced the tumor burden in Panc02 tumor-bearing mice by increasing the pro-inflammatory macrophages, which exhibited anti-tumor function [205]. Golubovskaya et al. showed that CD47 blockade could reduce tumor growth in BxPC-3 tumor-bearing mice [206]. Cioffi et al. demonstrated that a combination of CD47 inhibition and chemotherapy drugs resulted in reduced tumor growth, long-term prevention of tumor recurrence after discontinuation of treatment in the patient-derived xenograft model [207]. My results also indicated that CD47 blockade could significantly reduce the PSCs-mediated pro-tumorigenic effects on PCCs. Hence, CD47 is also a viable target for PDAC treatment.

Moreover, future research should also consider evaluating this therapeutic target with

new research models which can replicate as much as possible the conditions inside human PDAC (e.g., hypoxia, high intratumoral pressure). In addition, since every model has its own limitations, it needs to be thoroughly assessed in different models before we take them into clinical trials.

All in all, targeting the VDR/THBS1/CD47 axis is an effective therapeutic approach for PDAC treatment, and more research is also needed to expand our understanding of this axis.

5. Conclusion and Outlook

In summary, the VD analog Cal decreased PSCs-augmented proliferation, invasion, migration, and EMT of PCCs by downregulating THBS1, and this procedure was mediated by CD47. Figure 25 is a graphic summary of our project. Our work indicated that targeting VDR/THBS1/CD47 axis could be a promising strategy for PDAC therapy.

In the future, we will further validate the outcomes, which may involve but is not limited to: a) confirming these results in the PDAC mouse model or organoid model. b) analyzing the correlation between VDR/THBS1/CD47 axis and clinical outcomes based on clinical data of PDAC patients in our hospital.

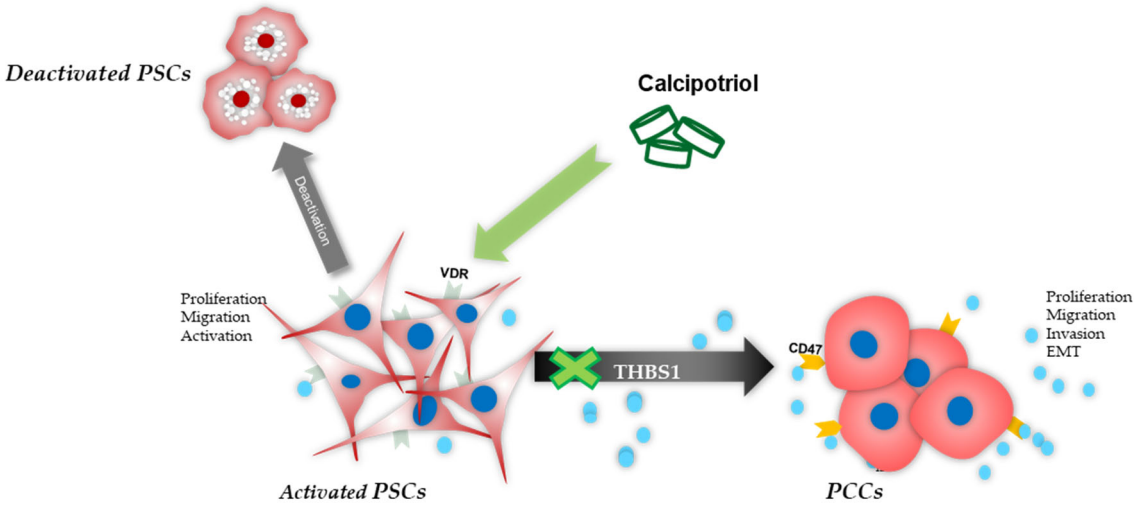

Figure 25: Graphic summary of our work. VD analog could deactivate PSCs and decrease PSCs-augmented PCCs aggressiveness by downregulating THBS1/ CD47 axis.

6. Summary

PDAC is a gastrointestinal malignancy with poor clinical outcomes. Accumulating evidence indicates that the crosstalk between PSCs and PCCs can establish a tumor-supportive stroma of PDAC, thereby enhancing tumor growth, metastasis, and chemoresistance. Recently, targeting PSCs has emerged as a promising strategy for PDAC therapy since standard chemotherapy has shown disappointing outcomes. Our previous work has demonstrated that the VD analog Cal can deactivate PSCs as well as the PSCs-augmented malignancy of PCCs. This project aims to investigate the role of the VDR/THBS1/CD47 axis in PSCs-PCCs crosstalk in vitro, which would provide a new target therapy for PDAC treatment.

Bioinformatic analysis showed that THBS1 and CD47 were highly expressed in PDAC and correlated with shorter disease-free survival. By ELISA, PSCs were shown to secret significantly higher expression of THBS1 than PCCs, and the VD analog Cal decreased THBS1 secretion in PSCs. PCCs treated with recombinant THBS1 exhibited promoted proliferation, migration, invasion, and EMT of PCCs. Furthermore, THBS1 neutralizing Ab and CD47 blocking Ab were applied to investigate the role of the VDR/THBS1/CD47 axis in the PSCs-PCCs crosstalk. Results showed that both antibodies decreased the PSCs-induced malignancy of PCCs (proliferation, migration, invasion, and EMT) utilizing EZ4U, WH test, transwell assay, and qRT-PCR.

In conclusion, Cal decreased PSCs-augmented proliferation, invasion, migration, and EMT of PCCs by downregulating THBS1, and this procedure was mediated by CD47. Our work indicated that targeting VDR/THBS1/CD47 axis could be a promising strategy for PDAC therapy.

7. Zusammenfassung

Das Pankreaskarzinom gilt als einer der bösartigsten Tumoren des Gastrointestinaltraktes und ist mit einer sehr schlechten Prognose vergesellschaftet. Es gilt hierbei als gesichert, dass das Tumorstroma ein wichtiger Mediator der Progression des Pankreaskarzinoms darstellt. Hierbei kommt es zu Wechselwirkungen zwischen den stromalen pankreatischen Stellatumzellen (PSCs) und den Pankreaskarzinomzellen (PCCs), wodurch das Tumorwachstum, die Metastasierung und die Chemoresistenz beeinflusst werden können. Die gezielte Behandlung dieser Stellatumzellen stellt somit eine vielversprechende Strategie zur Behandlung des Pankreaskarzinoms dar. In unseren Vorarbeiten konnten wir zeigen, dass Vitamin-D-Analoga die durch Stellatumzellen verstärkten Malignitätsmerkmale von Pankreaskarzinomuzellen verringern kann. Dieses Anschlussprojekt zielte darauf ab, die Rolle und das therapeutische Potential des Vitamin D Rezeptors, sowie des THBS1-CD47-Signalweges bei der Interaktion zwischen PSCs und PCCs in vitro zu untersuchen.

In einer bioinformatischen Analyse der STRING Datenbank konnten wir zeigen, dass THBS1 und CD47 im Pankreaskarzinom deutlich überexprimiert werden und mit einem kürzeren krankheitsfreien Überleben korrelieren. In dieser Arbeit konnte die Überexpression von THBS1 mittels ELISA-Assay in Pankreaskarzinomzellen bestätigt und gezeigt werden, dass diese Vitamin-D abhängig ist. Die mit Vitamin-D Analogon behandelten Zellen zeigten eine verringerte THBS1 Sekretion. Darüber hinaus zeigte sich eine gesteigerte Proliferation, Migration, Invasion und EMT in PCCs nach Stimulation mit rekombinantem THBS1. Zuletzt konnte durch den Einsatz von sowohl THBS1 neutralisierenden Antikörpern als auch CD47-blockierenden Antikörpern die Stellatumzell-induzierten Malignitätsmerkmale von Pankreaskarzinomzellen signifikant reduziert werden.

Zusammenfassend lässt sich zeigen, dass die Stimulation der pankreatischen Stellatumzellen mit einem Vitamin-D Analogon über einer Herunterregulation von THBS1, vermittelt über den Rezeptor CD47, zu einer verminderten Proliferation, Invasion, Migration und EMT der Pankreaskarzinomzellen führt. Die vorliegende Arbeit demonstriert somit, dass die Vitamin-D-Rezeptor/THBS1/CD47-Achse ein vielversprechendes Ziel für eine zukünftige anti-tumorale Modulation des Tumorstromas und damit für die Therapie des Pankreaskarzinoms darstellt.

III. Reference

1. Siegel, R.L., K.D. Miller, and A. Jemal, *Cancer statistics, 2019.* CA Cancer J Clin, 2019. **69**(1): p. 7-34.

2. McGuire, S., *World Cancer Report 2014. Geneva, Switzerland: World Health Organization, International Agency for Research on Cancer, WHO Press, 2015.* Adv Nutr, 2016. **7**(2): p. 418-9.

3. Tempero, M.A., et al., *Pancreatic Adenocarcinoma, Version 1.2019.* J Natl Compr Canc Netw, 2019. **17**(3): p. 202-210.

4. Apte, M.V., et al., *Desmoplastic reaction in pancreatic cancer - Role of pancreatic stellate cells.* Pancreas, 2004. **29**(3): p. 179-187.

5. Vonlaufen, A., et al., *Pancreatic stellate cells and pancreatic cancer cells: An unholy alliance.* Cancer Research, 2008. **68**(19): p. 7707-7710.

6. Erkan, M., et al., *StellaTUM: current consensus and discussion on pancreatic stellate cell research.* Gut, 2012. **61**(2): p. 172-178.

7. Apte, M.V., et al., *A Starring Role for Stellate Cells in the Pancreatic Cancer Microenvironment.* Gastroenterology, 2013. **144**(6): p. 1210-1219.

8. Tzilas, V., et al., *Vitamin D prevents experimental lung fibrosis and predicts survival in patients with idiopathic pulmonary fibrosis.* Pulm Pharmacol Ther, 2019. **55**: p. 17-24.

9. He, X., et al., *MicroRNA-351 promotes schistosomiasis-induced hepatic fibrosis by targeting the vitamin D receptor.* Proc Natl Acad Sci U S A, 2018. **115**(1): p. 180-185.

10. Duran, A., et al., *p62/SQSTM1 by Binding to Vitamin D Receptor Inhibits Hepatic Stellate Cell Activity, Fibrosis, and Liver Cancer.* Cancer Cell, 2016. **30**(4): p. 595-609.

11. Tian, Y., et al., *Effects of vitamin D on renal fibrosis in diabetic nephropathy*

model rats. Int J Clin Exp Pathol, 2014. **7**(6): p. 3028-37.

12. Ding, N., et al., *A vitamin D receptor/SMAD genomic circuit gates hepatic fibrotic response.* Cell, 2013. **153**(3): p. 601-13.

13. Bray, F., et al., *Global cancer statistics 2018: GLOBOCAN estimates of incidence and mortality worldwide for 36 cancers in 185 countries.* CA Cancer J Clin, 2018. **68**(6): p. 394-424.

14. Ferlay J, E.M., Lam F, Colombet M, Mery L, Piñeros M, Znaor A, Soerjomataram I, Bray F. *Global cancer observatory: cancer today*. 2018.

15. Ilic, M. and I. Ilic, *Epidemiology of pancreatic cancer.* World J Gastroenterol, 2016. **22**(44): p. 9694-9705.

16. Ferlay, J., C. Partensky, and F. Bray, *More deaths from pancreatic cancer than breast cancer in the EU by 2017.* Acta Oncol, 2016. **55**(9-10): p. 1158-1160.

17. Dauer, P., et al., *Microenvironment in determining chemo-resistance in pancreatic cancer: Neighborhood matters.* Pancreatology, 2017. **17**(1): p. 7-12.

18. Lindsey, S. and S.A. Langhans, *Crosstalk of Oncogenic Signaling Pathways during Epithelial-Mesenchymal Transition.* Front Oncol, 2014. **4**: p. 358.

19. Bynigeri, R.R., et al., *Pancreatic stellate cell: Pandora's box for pancreatic disease biology.* World J Gastroenterol, 2017. **23**(3): p. 382-405.

20. Kupffer, K.v., *Ueber Sternzellen der Leber. Briefliche Mitteilung an Prof. Waldyer.* Arch mikr Anat 1876. **12:353-358.**

21. Watari, N., Y. Hotta, and Y. Mabuchi, *Morphological studies on a vitamin A-storing cell and its complex with macrophage observed in mouse pancreatic tissues following excess vitamin A administration.* Okajimas Folia Anat Jpn, 1982. **58**(4-6): p. 837-58.

22. Apte, M.V., et al., *Periacinar stellate shaped cells in rat pancreas: identification, isolation, and culture.* Gut, 1998. **43**(1): p. 128-133.

23. Bachem, M.G., et al., *Identification, culture, and characterization of pancreatic stellate cells in rats and humans.* Gastroenterology, 1998. **115**(2): p. 421-432.

24. Apte, M.V. and J.S. Wilson, *Mechanisms of pancreatic fibrosis.* Digestive Diseases, 2004. **22**(3): p. 273-279.

25. Mews, P., et al., *Pancreatic stellate cells respond to inflammatory cytokines: potential role in chronic pancreatitis.* Gut, 2002. **50**(4): p. 535-541.

26. Haber, P.S., et al., *Activation of pancreatic stellate cells in human and experimental pancreatic fibrosis.* American Journal of Pathology, 1999. **155**(4): p. 1087-1095.

27. Duner, S., et al., *Pancreatic Cancer: The Role of Pancreatic Stellate Cells in Tumor Progression.* Pancreatology, 2010. **10**(6): p. 673-681.

28. Allam, A., et al., *Pancreatic stellate cells in pancreatic cancer: In focus.* Pancreatology, 2017. **17**(4): p. 514-522.

29. Bynigeri, R.R., et al., *Pancreatic stellate cell: Pandora's box for pancreatic disease biology.* World Journal of Gastroenterology, 2017. **23**(3): p. 382-405.

30. Apte, M.V., et al., *Pancreatic stellate cells are activated by proinflammatory cytokines: implications for pancreatic fibrogenesis.* Gut, 1999. **44**(4): p. 534-541.

31. Porembka, M.R., et al., *Pancreatic adenocarcinoma induces bone marrow mobilization of myeloid-derived suppressor cells which promote primary tumor growth.* Cancer Immunol Immunother, 2012. **61**(9): p. 1373-85.

32. Diaz-Montero, C.M., et al., *Increased circulating myeloid-derived suppressor cells correlate with clinical cancer stage, metastatic tumor burden, and doxorubicin-cyclophosphamide chemotherapy.* Cancer Immunol Immunother, 2009. **58**(1): p. 49-59.

33. Liu, G., et al., *SIRT1 limits the function and fate of myeloid-derived suppressor cells in tumors by orchestrating HIF-1alpha-dependent glycolysis.* Cancer Res, 2014. **74**(3): p. 727-37.

34. Corzo, C.A., et al., *Mechanism regulating reactive oxygen species in tumor-induced myeloid-derived suppressor cells.* J Immunol, 2009. **182**(9): p. 5693-701.

35. Pinton, L., et al., *Activated T cells sustain myeloid-derived suppressor cell-*

mediated immune suppression. Oncotarget, 2016. **7**(2): p. 1168-84.

36. Huang, B., et al., *Gr-1+CD115+ immature myeloid suppressor cells mediate the development of tumor-induced T regulatory cells and T-cell anergy in tumor-bearing host.* Cancer Res, 2006. **66**(2): p. 1123-31.

37. Kumar, V., et al., *CD45 Phosphatase Inhibits STAT3 Transcription Factor Activity in Myeloid Cells and Promotes Tumor-Associated Macrophage Differentiation.* Immunity, 2016. **44**(2): p. 303-15.

38. Looi, C.K., et al., *Therapeutic challenges and current immunomodulatory strategies in targeting the immunosuppressive pancreatic tumor microenvironment.* J Exp Clin Cancer Res, 2019. **38**(1): p. 162.

39. Lankadasari, M.B., et al., *TAMing pancreatic cancer: combat with a double edged sword.* Mol Cancer, 2019. **18**(1): p. 48.

40. Condeelis, J. and J.W. Pollard, *Macrophages: obligate partners for tumor cell migration, invasion, and metastasis.* Cell, 2006. **124**(2): p. 263-6.

41. Coffelt, S.B., R. Hughes, and C.E. Lewis, *Tumor-associated macrophages: effectors of angiogenesis and tumor progression.* Biochim Biophys Acta, 2009. **1796**(1): p. 11-8.

42. Joyce, J.A. and J.W. Pollard, *Microenvironmental regulation of metastasis.* Nat Rev Cancer, 2009. **9**(4): p. 239-52.

43. Kurahara, H., et al., *Significance of M2-polarized tumor-associated macrophage in pancreatic cancer.* J Surg Res, 2011. **167**(2): p. e211-9.

44. Chen, S.J., et al., *Distribution and clinical significance of tumour-associated macrophages in pancreatic ductal adenocarcinoma: a retrospective analysis in China.* Curr Oncol, 2015. **22**(1): p. e11-9.

45. Noy, R. and J.W. Pollard, *Tumor-associated macrophages: from mechanisms to therapy.* Immunity, 2014. **41**(1): p. 49-61.

46. Ben-Baruch, A., *Inflammation-associated immune suppression in cancer: the roles played by cytokines, chemokines and additional mediators.* Semin Cancer Biol, 2006. **16**(1): p. 38-52.

47. Liou, G.Y., et al., *The Presence of Interleukin-13 at Pancreatic ADM/PanIN Lesions Alters Macrophage Populations and Mediates Pancreatic Tumorigenesis.* Cell Rep, 2017. **19**(7): p. 1322-1333.

48. Meng, F., et al., *Interaction between pancreatic cancer cells and tumor-associated macrophages promotes the invasion of pancreatic cancer cells and the differentiation and migration of macrophages.* IUBMB Life, 2014. **66**(12): p. 835-46.

49. Farran, B. and G.P. Nagaraju, *The dynamic interactions between the stroma, pancreatic stellate cells and pancreatic tumor development: Novel therapeutic targets.* Cytokine Growth Factor Rev, 2019. **48**: p. 11-23.

50. Xiao, Y., et al., *YAP1-mediated pancreatic stellate cell activation inhibits pancreatic cancer cell proliferation.* Cancer Lett, 2019. **462**: p. 51-60.

51. Horioka, K., et al., *Suppression of CD51 in pancreatic stellate cells inhibits tumor growth by reducing stroma and altering tumor-stromal interaction in pancreatic cancer.* Int J Oncol, 2016. **48**(4): p. 1499-508.

52. Dalin, S., et al., *Deoxycytidine Release from Pancreatic Stellate Cells Promotes Gemcitabine Resistance.* Cancer Res, 2019. **79**(22): p. 5723-5733.

53. Wen, Z., et al., *Fibroblast activation protein alpha-positive pancreatic stellate cells promote the migration and invasion of pancreatic cancer by CXCL1-mediated Akt phosphorylation.* Ann Transl Med, 2019. **7**(20): p. 532.

54. Kuninty, P.R., et al., *ITGA5 inhibition in pancreatic stellate cells attenuates desmoplasia and potentiates efficacy of chemotherapy in pancreatic cancer.* Sci Adv, 2019. **5**(9): p. eaax2770.

55. Yuan, Y., et al., *BAG3-positive pancreatic stellate cells promote migration and invasion of pancreatic ductal adenocarcinoma.* J Cell Mol Med, 2019. **23**(8): p. 5006-5016.

56. Junliang, L., et al., *High-molecular-weight hyaluronan produced by activated pancreatic stellate cells promotes pancreatic cancer cell migration via paracrine signaling.* Biochem Biophys Res Commun, 2019. **515**(3): p. 493-498.

57. Hwang, H.J., et al., *Multiplex quantitative analysis of stroma-mediated cancer cell invasion, matrix remodeling, and drug response in a 3D co-culture model*

of pancreatic tumor spheroids and stellate cells. J Exp Clin Cancer Res, 2019. **38**(1): p. 258.

58. Wang, H.C., et al., *Pancreatic stellate cells activated by mutant KRAS-mediated PAI-1 upregulation foster pancreatic cancer progression via IL-8.* Theranostics, 2019. **9**(24): p. 7168-7183.

59. Nan, L., et al., *Pancreatic Stellate Cells Facilitate Perineural Invasion of Pancreatic Cancer via HGF/c-Met Pathway.* Cell Transplant, 2019. **28**(9-10): p. 1289-1298.

60. Tang, D., et al., *Identification of key pathways and gene changes in primary pancreatic stellate cells after cross-talk with pancreatic cancer cells (BXPC-3) using bioinformatics analysis.* Neoplasma, 2019. **66**(3): p. 446-458.

61. Zhou, L., et al., *Suppression of stromal-derived Dickkopf-3 (DKK3) inhibits tumor progression and prolongs survival in pancreatic ductal adenocarcinoma.* Sci Transl Med, 2018. **10**(464).

62. Chu, G.C., et al., *Stromal biology of pancreatic cancer.* J Cell Biochem, 2007. **101**(4): p. 887-907.

63. Vennin, C., et al., *Reshaping the Tumor Stroma for Treatment of Pancreatic Cancer.* Gastroenterology, 2018. **154**(4): p. 820-838.

64. Neesse, A., et al., *Stromal biology and therapy in pancreatic cancer: ready for clinical translation?* Gut, 2019. **68**(1): p. 159-171.

65. Yang Wu, C.Z., Kuirong Jiang, Jens Werner, Alexandr Bazhin1 and Jan G. D'haese, *The role of stellate cells in pancreatic ductal adenocarcinoma: targeting perspectives.* Frontiers in Oncology, 2020.

66. McCarroll, J.A., et al., *Role of pancreatic stellate cells in chemoresistance in pancreatic cancer.* Front Physiol, 2014. **5**: p. 141.

67. Berchtold, S., et al., *Collagen type V promotes the malignant phenotype of pancreatic ductal adenocarcinoma.* Cancer Lett, 2015. **356**(2 Pt B): p. 721-32.

68. Di Maggio, F., et al., *Pancreatic stellate cells regulate blood vessel density in the stroma of pancreatic ductal adenocarcinoma.* Pancreatology, 2016. **16**(6): p. 995-1004.

69. Provenzano, P.P., et al., *Enzymatic targeting of the stroma ablates physical barriers to treatment of pancreatic ductal adenocarcinoma.* Cancer Cell, 2012. **21**(3): p. 418-29.

70. Schnittert, J., R. Bansal, and J. Prakash, *Targeting Pancreatic Stellate Cells in Cancer.* Trends Cancer, 2019. **5**(2): p. 128-142.

71. Halbrook, C.J. and C.A. Lyssiotis, *Employing Metabolism to Improve the Diagnosis and Treatment of Pancreatic Cancer.* Cancer Cell, 2017. **31**(1): p. 5-19.

72. Sousa, C.M., et al., *Pancreatic stellate cells support tumour metabolism through autophagic alanine secretion.* Nature, 2016. **536**(7617): p. 479-83.

73. Tape, C.J., et al., *Oncogenic KRAS Regulates Tumor Cell Signaling via Stromal Reciprocation.* Cell, 2016. **165**(4): p. 910-20.

74. Zhao, H., et al., *Tumor microenvironment derived exosomes pleiotropically modulate cancer cell metabolism.* Elife, 2016. **5**: p. e10250.

75. Hessmann, E., et al., *Fibroblast drug scavenging increases intratumoural gemcitabine accumulation in murine pancreas cancer.* Gut, 2018. **67**(3): p. 497-507.

76. Buckway, B., et al., *Overcoming the stromal barrier for targeted delivery of HPMA copolymers to pancreatic tumors.* Int J Pharm, 2013. **456**(1): p. 202-11.

77. Cao, F., et al., *HES 1 is essential for chemoresistance induced by stellate cells and is associated with poor prognosis in pancreatic cancer.* Oncol Rep, 2015. **33**(4): p. 1883-9.

78. Liu, Y., et al., *Periostin promotes the chemotherapy resistance to gemcitabine in pancreatic cancer.* Tumour Biol, 2016. **37**(11): p. 15283-15291.

79. Singh, S., et al., *CXCL12-CXCR4 signalling axis confers gemcitabine resistance to pancreatic cancer cells: a novel target for therapy.* Br J Cancer, 2010. **103**(11): p. 1671-9.

80. Zhang, H., et al., *Paracrine SDF-1alpha signaling mediates the effects of PSCs on GEM chemoresistance through an IL-6 autocrine loop in pancreatic cancer cells.* Oncotarget, 2015. **6**(5): p. 3085-97.

81. Amrutkar, M., et al., *Secretion of fibronectin by human pancreatic stellate cells promotes chemoresistance to gemcitabine in pancreatic cancer cells.* BMC Cancer, 2019. **19**(1): p. 596.

82. Richards, K.E., et al., *Cancer-associated fibroblast exosomes regulate survival and proliferation of pancreatic cancer cells.* Oncogene, 2017. **36**(13): p. 1770-1778.

83. Tang, D., et al., *Persistent activation of pancreatic stellate cells creates a microenvironment favorable for the malignant behavior of pancreatic ductal adenocarcinoma.* Int J Cancer, 2013. **132**(5): p. 993-1003.

84. Kikuta, K., et al., *Pancreatic stellate cells promote epithelial-mesenchymal transition in pancreatic cancer cells.* Biochemical and Biophysical Research Communications, 2010. **403**(3-4): p. 380-384.

85. Neesse, A., et al., *Pancreatic stellate cells potentiate proinvasive effects of SERPINE2 expression in pancreatic cancer xenograft tumors.* Pancreatology, 2007. **7**(4): p. 380-5.

86. Tian, X., et al., *Interactions of pancreatic cancer and stellate cells are mediated by FGFR1-III isoform expression.* Hepatogastroenterology, 2012. **59**(117): p. 1604-8.

87. Xu, Z.H., et al., *Role of Pancreatic Stellate Cells in Pancreatic Cancer Metastasis.* American Journal of Pathology, 2010. **177**(5): p. 2585-2596.

88. Suetsugu, A., et al., *Imaging the Interaction of Pancreatic Cancer and Stellate Cells in the Tumor Microenvironment during Metastasis.* Anticancer Res, 2015. **35**(5): p. 2545-51.

89. Paget, S., *The distribution of secondary growths in cancer of the breast. 1889.* Cancer Metastasis Rev, 1989. **8**(2): p. 98-101.

90. Pang, T.C.Y., et al., *Circulating pancreatic stellate (stromal) cells in pancreatic cancer-a fertile area for novel research.* Carcinogenesis, 2017. **38**(6): p. 588-591.

91. Gao, Z., et al., *Pancreatic stellate cells increase the invasion of human pancreatic cancer cells through the stromal cell-derived factor-1/CXCR4 axis.* Pancreatology, 2010. **10**(2-3): p. 186-93.

92. Zhao, W., et al., *Galectin-3 Mediates Tumor Cell-Stroma Interactions by Activating Pancreatic Stellate Cells to Produce Cytokines via Integrin Signaling.* Gastroenterology, 2018. **154**(5): p. 1524-1537 e6.

93. Yang, X.P., et al., *Pancreatic stellate cells increase pancreatic cancer cells invasion through the hepatocyte growth factor /c-Met/survivin regulated by P53/P21.* Exp Cell Res, 2017. **357**(1): p. 79-87.

94. Nagathihalli, N.S., et al., *Pancreatic stellate cell secreted IL-6 stimulates STAT3 dependent invasiveness of pancreatic intraepithelial neoplasia and cancer cells.* Oncotarget, 2016. **7**(40): p. 65982-65992.

95. Farrow, B., D.H. Berger, and D. Rowley, *Tumor-derived pancreatic stellate cells promote pancreatic cancer cell invasion through release of thrombospondin-2.* J Surg Res, 2009. **156**(1): p. 155-60.

96. Li, Y., et al., *Pancreatic Stellate Cells Activation and Matrix Metallopeptidase 2 Expression Correlate With Lymph Node Metastasis in Pancreatic Carcinoma.* Am J Med Sci, 2019. **357**(1): p. 16-22.

97. Zhou, Y., Q. Zhou, and R. Chen, *Pancreatic stellate cells promotes the perineural invasion in pancreatic cancer.* Med Hypotheses, 2012. **78**(6): p. 811-3.

98. Schnittert, J., et al., *Integrin alpha11 in pancreatic stellate cells regulates tumor stroma interaction in pancreatic cancer.* FASEB J, 2019. **33**(5): p. 6609-6621.

99. Qian, D., et al., *Galectin-1-driven upregulation of SDF-1 in pancreatic stellate cells promotes pancreatic cancer metastasis.* Cancer Lett, 2017. **397**: p. 43-51.

100. Pothula, S.P., et al., *Targeting the HGF/c-MET pathway: stromal remodelling in pancreatic cancer.* Oncotarget, 2017. **8**(44): p. 76722-76739.

101. Pothula, S.P., et al., *Hepatocyte growth factor inhibition: a novel therapeutic approach in pancreatic cancer.* Br J Cancer, 2016. **114**(3): p. 269-80.

102. Tang, D., et al., *High expression of Galectin-1 in pancreatic stellate cells plays a role in the development and maintenance of an immunosuppressive microenvironment in pancreatic cancer.* Int J Cancer, 2012. **130**(10): p. 2337-48.

103. Incio, J., et al., *Obesity-Induced Inflammation and Desmoplasia Promote Pancreatic Cancer Progression and Resistance to Chemotherapy.* Cancer Discov, 2016. **6**(8): p. 852-69.

104. Gabitass, R.F., et al., *Elevated myeloid-derived suppressor cells in pancreatic, esophageal and gastric cancer are an independent prognostic factor and are associated with significant elevation of the Th2 cytokine interleukin-13.* Cancer Immunol Immunother, 2011. **60**(10): p. 1419-30.

105. Markowitz, J., et al., *Patients with pancreatic adenocarcinoma exhibit elevated levels of myeloid-derived suppressor cells upon progression of disease.* Cancer Immunol Immunother, 2015. **64**(2): p. 149-59.

106. Ene-Obong, A., et al., *Activated pancreatic stellate cells sequester CD8+ T cells to reduce their infiltration of the juxtatumoral compartment of pancreatic ductal adenocarcinoma.* Gastroenterology, 2013. **145**(5): p. 1121-32.

107. Wu, Q., et al., *Functions of pancreatic stellate cell-derived soluble factors in the microenvironment of pancreatic ductal carcinoma.* Oncotarget, 2017. **8**(60): p. 102721-102738.

108. Mace, T.A., M. Bloomston, and G.B. Lesinski, *Pancreatic cancer-associated stellate cells: A viable target for reducing immunosuppression in the tumor microenvironment.* Oncoimmunology, 2013. **2**(7): p. e24891.

109. Lunardi, S., et al., *IP-10/CXCL10 induction in human pancreatic cancer stroma influences lymphocytes recruitment and correlates with poor survival.* Oncotarget, 2014. **5**(22): p. 11064-80.

110. Tang, D., et al., *Persistent activation of pancreatic stellate cells creates a microenvironment favorable for the malignant behavior of pancreatic ductal adenocarcinoma.* International Journal of Cancer, 2013. **132**(5): p. 993-1003.

111. Kuninty, P.R., et al., *MicroRNA-199a and -214 as potential therapeutic targets in pancreatic stellate cells in pancreatic tumor.* Oncotarget, 2016. **7**(13): p. 16396-408.

112. Patel, M.B., et al., *The role of the hepatocyte growth factor/c-MET pathway in pancreatic stellate cell-endothelial cell interactions: antiangiogenic implications in pancreatic cancer.* Carcinogenesis, 2014. **35**(8): p. 1891-900.

113. Li, X., et al., *Sonic hedgehog paracrine signaling activates stromal cells to promote perineural invasion in pancreatic cancer.* Clin Cancer Res, 2014. **20**(16): p. 4326-38.

114. Han, L., et al., *Pancreatic stellate cells contribute pancreatic cancer pain via activation of sHH signaling pathway.* Oncotarget, 2016. **7**(14): p. 18146-58.

115. Demir, I.E., et al., *The microenvironment in chronic pancreatitis and pancreatic cancer induces neuronal plasticity.* Neurogastroenterol Motil, 2010. **22**(4): p. 480-90, e112-3.

116. Whatcott, C.J., et al., *Inhibition of ROCK1 kinase modulates both tumor cells and stromal fibroblasts in pancreatic cancer.* PLoS One, 2017. **12**(8): p. e0183871.

117. Zhang, Y., et al., *Vitamin A-coupled liposomes carrying TLR4-silencing shRNA induce apoptosis of pancreatic stellate cells and resolution of pancreatic fibrosis.* J Mol Med (Berl), 2018. **96**(5): p. 445-458.

118. Yeo, D., et al., *Inhibition of group 1 p21-activated kinases suppresses pancreatic stellate cell activation and increases survival of mice with pancreatic cancer.* Int J Cancer, 2017. **140**(9): p. 2101-2111.

119. Ozdemir, B.C., et al., *Depletion of Carcinoma-Associated Fibroblasts and Fibrosis Induces Immunosuppression and Accelerates Pancreas Cancer with Reduced Survival.* Cancer Cell, 2015. **28**(6): p. 831-833.

120. Prakash, J., *Cancer-Associated Fibroblasts: Perspectives in Cancer Therapy.* Trends Cancer, 2016. **2**(6): p. 277-279.

121. Schnittert, J., et al., *Reprogramming tumor stroma using an endogenous lipid lipoxin A4 to treat pancreatic cancer.* Cancer Lett, 2018. **420**: p. 247-258.

122. Sherman, M.H., et al., *Vitamin D Receptor-Mediated Stromal Reprogramming Suppresses Pancreatitis and Enhances Pancreatic Cancer Therapy.* Cell, 2014. **159**(1): p. 80-93.

123. Froeling, F.E.M., et al., *Retinoic Acid-Induced Pancreatic Stellate Cell Quiescence Reduces Paracrine Wnt-beta-Catenin Signaling to Slow Tumor Progression.* Gastroenterology, 2011. **141**(4): p. 1486-U503.

124. Olive, K.P., et al., *Inhibition of Hedgehog signaling enhances delivery of chemotherapy in a mouse model of pancreatic cancer.* Science, 2009. **324**(5933): p. 1457-61.

125. Rhim, A.D., et al., *Stromal Elements Act to Restrain, Rather Than Support, Pancreatic Ductal Adenocarcinoma.* Cancer Cell, 2014. **25**(6): p. 735-747.

126. Amakye, D., Z. Jagani, and M. Dorsch, *Unraveling the therapeutic potential of the Hedgehog pathway in cancer.* Nat Med, 2013. **19**(11): p. 1410-22.

127. Hwang, R.F., et al., *Inhibition of the hedgehog pathway targets the tumor-associated stroma in pancreatic cancer.* Mol Cancer Res, 2012. **10**(9): p. 1147-57.

128. Jaster, R., et al., *Regulation of pancreatic stellate cell function in vitro: biological and molecular effects of all-trans retinoic acid.* Biochem Pharmacol, 2003. **66**(4): p. 633-41.

129. McCarroll, J.A., et al., *Vitamin A inhibits pancreatic stellate cell activation: implications for treatment of pancreatic fibrosis.* Gut, 2006. **55**(1): p. 79-89.

130. Han, X., et al., *Reversal of pancreatic desmoplasia by re-educating stellate cells with a tumour microenvironment-activated nanosystem.* Nat Commun, 2018. **9**(1): p. 3390.

131. Michael, A., et al., *13-cis-Retinoic acid in combination with gemcitabine in the treatment of locally advanced and metastatic pancreatic cancer--report of a pilot phase II study.* Clin Oncol (R Coll Radiol), 2007. **19**(2): p. 150-3.

132. Moore, D.F., Jr., et al., *Pilot phase II trial of 13-cis-retinoic acid and interferon-alpha combination therapy for advanced pancreatic adenocarcinoma.* Am J Clin Oncol, 1995. **18**(6): p. 525-7.

133. Kocher, H.M., et al., *Phase I clinical trial repurposing all-trans retinoic acid as a stromal targeting agent for pancreatic cancer.* Nat Commun, 2020. **11**(1): p. 4841.

134. Kota, J., et al., *Pancreatic cancer: Stroma and its current and emerging targeted therapies.* Cancer Lett, 2017. **391**: p. 38-49.

135. Masamune, A., et al., *The angiotensin II type I receptor blocker olmesartan*

inhibits the growth of pancreatic cancer by targeting stellate cell activities in mice. Scand J Gastroenterol, 2013. **48**(5): p. 602-9.

136. Chauhan, V.P., et al., *Angiotensin inhibition enhances drug delivery and potentiates chemotherapy by decompressing tumour blood vessels.* Nat Commun, 2013. **4**: p. 2516.

137. Kozono, S., et al., *Pirfenidone inhibits pancreatic cancer desmoplasia by regulating stellate cells.* Cancer Res, 2013. **73**(7): p. 2345-56.

138. Suklabaidya, S., et al., *Characterization and use of HapT1-derived homologous tumors as a preclinical model to evaluate therapeutic efficacy of drugs against pancreatic tumor desmoplasia.* Oncotarget, 2016. **7**(27): p. 41825-41842.

139. Kuninty, P.R., et al., *MicroRNA Targeting to Modulate Tumor Microenvironment.* Front Oncol, 2016. **6**: p. 3.

140. Kwon, J.J., et al., *Pathophysiological role of microRNA-29 in pancreatic cancer stroma.* Sci Rep, 2015. **5**: p. 11450.

141. Asama, H., et al., *MicroRNA let-7d targets thrombospondin-1 and inhibits the activation of human pancreatic stellate cells.* Pancreatology, 2019. **19**(1): p. 196-203.

142. Orozco, C.A., et al., *Targeting galectin-1 inhibits pancreatic cancer progression by modulating tumor-stroma crosstalk.* Proc Natl Acad Sci U S A, 2018. **115**(16): p. E3769-E3778.

143. Jacobetz, M.A., et al., *Hyaluronan impairs vascular function and drug delivery in a mouse model of pancreatic cancer.* Gut, 2013. **62**(1): p. 112-20.

144. Hingorani, S.R., et al., *Phase Ib Study of PEGylated Recombinant Human Hyaluronidase and Gemcitabine in Patients with Advanced Pancreatic Cancer.* Clin Cancer Res, 2016. **22**(12): p. 2848-54.

145. Hingorani, S.R., et al., *HALO 202: Randomized Phase II Study of PEGPH20 Plus Nab-Paclitaxel/Gemcitabine Versus Nab-Paclitaxel/Gemcitabine in Patients With Untreated, Metastatic Pancreatic Ductal Adenocarcinoma.* J Clin Oncol, 2018. **36**(4): p. 359-366.

146. Tao, Q., et al., *Vitamin D prevents the intestinal fibrosis via induction of vitamin*

D receptor and inhibition of transforming growth factor-beta1/Smad3 pathway. Dig Dis Sci, 2015. **60**(4): p. 868-75.

147. Pattanaik, D., et al., *Pathogenesis of Systemic Sclerosis.* Front Immunol, 2015. **6**: p. 272.

148. Potter, J.J., et al., *1,25-dihydroxyvitamin D3 and its nuclear receptor repress human alpha1 (I) collagen expression and type I collagen formation.* Liver Int, 2013. **33**(5): p. 677-86.

149. Lichtler, A., et al., *Isolation and characterization of the rat alpha 1(I) collagen promoter. Regulation by vitamin D.* J Biol Chem, 1994. **269**(23): p. 16518.

150. Puche, J.E., Y. Saiman, and S.L. Friedman, *Hepatic Stellate Cells and Liver Fibrosis.* Comprehensive Physiology, 2013. **3**(4): p. 1473-1492.

151. Hellerbrand, C., *Hepatic stellate cells--the pericytes in the liver.* Pflugers Arch, 2013. **465**(6): p. 775-8.

152. Abramovitch, S., et al., *Vitamin D inhibits proliferation and profibrotic marker expression in hepatic stellate cells and decreases thioacetamide-induced liver fibrosis in rats.* Gut, 2011. **60**(12): p. 1728-1737.

153. Zerr, P., et al., *Vitamin D receptor regulates TGF-beta signalling in systemic sclerosis.* Annals of the Rheumatic Diseases, 2015. **74**(3).

154. Meredith, A., et al., *1,25 Dihydroxyvitamin D3 Inhibits TGFbeta1-Mediated Primary Human Cardiac Myofibroblast Activation.* PLoS One, 2015. **10**(6): p. e0128655.

155. Ding, N., et al., *A Vitamin D Receptor/SMAD Genomic Circuit Gates Hepatic Fibrotic Response.* Cell, 2013. **153**(3): p. 601-613.

156. Kong, F., et al., *VDR signaling inhibits cancer-associated-fibroblasts' release of exosomal miR-10a-5p and limits their supportive effects on pancreatic cancer cells.* Gut, 2019. **68**(5): p. 950-951.

157. Perez, K., et al., *Vitamin D receptor agonist paricalcitol plus gemcitabine and nab-paclitaxel in patients with metastatic pancreatic cancer.* Journal of Clinical Oncology, 2020. **38**(4_suppl): p. TPS784-TPS784.

158. JG D'Haese, Y.W., M less, M Illmer, J Werner, AV Bazhin, *Vitamin D beeinflusst die Migration und Aktivierung von pankreatischen Stellatumzellen und damit die Tumor-Stroma Interaktion im Pankreaskarzinom.* Zeitschrift für Gastroenterologie, 2019. **2019; 57(09): e311**.

159. Vonlaufen, A., et al., *Isolation of quiescent human pancreatic stellate cells: a promising in vitro tool for studies of human pancreatic stellate cell biology.* Pancreatology, 2010. **10**(4): p. 434-43.

160. Szklarczyk, D., et al., *STRING v11: protein-protein association networks with increased coverage, supporting functional discovery in genome-wide experimental datasets.* Nucleic Acids Res, 2019. **47**(D1): p. D607-D613.

161. Tang, Z., et al., *GEPIA: a web server for cancer and normal gene expression profiling and interactive analyses.* Nucleic Acids Res, 2017. **45**(W1): p. W98-W102.

162. Wehr, A.Y., et al., *Analysis of the human pancreatic stellate cell secreted proteome.* Pancreas, 2011. **40**(4): p. 557-66.

163. Guan, J., et al., *Retinoic acid inhibits pancreatic cancer cell migration and EMT through the downregulation of IL-6 in cancer associated fibroblast cells.* Cancer Lett, 2014. **345**(1): p. 132-9.

164. Mace, T.A., et al., *IL-6 and PD-L1 antibody blockade combination therapy reduces tumour progression in murine models of pancreatic cancer.* Gut, 2018. **67**(2): p. 320-332.

165. Yu, L., et al., *PSME3 Promotes TGFB1 Secretion by Pancreatic Cancer Cells to Induce Pancreatic Stellate Cell Proliferation.* J Cancer, 2019. **10**(9): p. 2128-2138.

166. Yee, K.O., et al., *The effect of thrombospondin-1 on breast cancer metastasis.* Breast Cancer Res Treat, 2009. **114**(1): p. 85-96.

167. Firlej, V., et al., *Thrombospondin-1 triggers cell migration and development of advanced prostate tumors.* Cancer Res, 2011. **71**(24): p. 7649-58.

168. Horiguchi, H., et al., *Thrombospondin-1 is highly expressed in desmoplastic components of invasive ductal carcinoma of the breast and associated with lymph node metastasis.* J Med Invest, 2013. **60**(1-2): p. 91-6.

169. Jayachandran, A., et al., *Thrombospondin 1 promotes an aggressive phenotype through epithelial-to-mesenchymal transition in human melanoma.* Oncotarget, 2014. **5**(14): p. 5782-97.

170. Borsotti, P., et al., *Thrombospondin-1 is part of a Slug-independent motility and metastatic program in cutaneous melanoma, in association with VEGFR-1 and FGF-2.* Pigment Cell Melanoma Res, 2015. **28**(1): p. 73-81.

171. Qian, X., et al., *Expression of thrombospondin-1 in human pancreatic adenocarcinomas: role in matrix metalloproteinase-9 production.* Pathol Oncol Res, 2001. **7**(4): p. 251-9.

172. Naganuma, H., et al., *Quantification of thrombospondin-1 secretion and expression of alphavbeta3 and alpha3beta1 integrins and syndecan-1 as cell-surface receptors for thrombospondin-1 in malignant glioma cells.* J Neurooncol, 2004. **70**(3): p. 309-17.

173. Kay, N.E., et al., *B-CLL cells are capable of synthesis and secretion of both pro- and anti-angiogenic molecules.* Leukemia, 2002. **16**(5): p. 911-9.

174. Jaffe, E.A., et al., *Cultured human fibroblasts synthesize and secrete thrombospondin and incorporate it into extracellular matrix.* Proc Natl Acad Sci U S A, 1983. **80**(4): p. 998-1002.

175. Raugi, G.J., et al., *Thrombospondin: synthesis and secretion by cells in culture.* J Cell Biol, 1982. **95**(1): p. 351-4.

176. Jeanne, A., et al., *Original insights on thrombospondin-1-related antireceptor strategies in cancer.* Front Pharmacol, 2015. **6**: p. 252.

177. Nucera, C., et al., *B-Raf(V600E) and thrombospondin-1 promote thyroid cancer progression.* Proc Natl Acad Sci U S A, 2010. **107**(23): p. 10649-54.

178. Xu, J., et al., *Paracrine HGF promotes EMT and mediates the effects of PSC on chemoresistance by activating c-Met/PI3K/Akt signaling in pancreatic cancer in vitro.* Life Sci, 2020: p. 118523.

179. Kikuta, K., et al., *Pancreatic stellate cells promote epithelial-mesenchymal transition in pancreatic cancer cells.* Biochem Biophys Res Commun, 2010. **403**(3-4): p. 380-4.

180. Kanno, A., et al., *Periostin, secreted from stromal cells, has biphasic effect on cell migration and correlates with the epithelial to mesenchymal transition of human pancreatic cancer cells.* Int J Cancer, 2008. **122**(12): p. 2707-18.

181. Karnevi, E., et al., *Impact by pancreatic stellate cells on epithelial-mesenchymal transition and pancreatic cancer cell invasion: Adding a third dimension in vitro.* Exp Cell Res, 2016. **346**(2): p. 206-15.

182. Wallbaum, P., et al., *Antifibrogenic effects of vitamin D derivatives on mouse pancreatic stellate cells.* World J Gastroenterol, 2018. **24**(2): p. 170-178.

183. Kang, Z.S., et al., *Design, synthesis and biological evaluation of non-secosteriodal vitamin D receptor ligand bearing double side chain for the treatment of chronic pancreatitis.* Eur J Med Chem, 2018. **146**: p. 541-553.

184. Blauer, M., J. Sand, and J. Laukkarinen, *Physiological and clinically attainable concentrations of 1,25-dihydroxyvitamin D3 suppress proliferation and extracellular matrix protein expression in mouse pancreatic stellate cells.* Pancreatology, 2015. **15**(4): p. 366-71.

185. Mahadevan, D. and D.D. Von Hoff, *Tumor-stroma interactions in pancreatic ductal adenocarcinoma.* Molecular Cancer Therapeutics, 2007. **6**(4): p. 1186-1197.

186. Omary, M.B., et al., *The pancreatic stellate cell: a star on the rise in pancreatic diseases.* Journal of Clinical Investigation, 2007. **117**(1): p. 50-59.

187. Erkan, M., et al., *The Activated Stroma Index Is a Novel and Independent Prognostic Marker in Pancreatic Ductal Adenocarcinoma.* Clinical Gastroenterology and Hepatology, 2008. **6**(10): p. 1155-1161.

188. Fu, Y., et al., *The critical roles of activated stellate cells-mediated paracrine signaling, metabolism and onco-immunology in pancreatic ductal adenocarcinoma.* Mol Cancer, 2018. **17**(1): p. 62.

189. Mutgan, A.C., et al., *Insulin/IGF-driven cancer cell-stroma crosstalk as a novel therapeutic target in pancreatic cancer.* Mol Cancer, 2018. **17**(1): p. 66.

190. Sid, B., et al., *Thrombospondin 1: a multifunctional protein implicated in the regulation of tumor growth.* Crit Rev Oncol Hematol, 2004. **49**(3): p. 245-58.

191. Leca, J., et al., *Cancer-associated fibroblast-derived annexin A6+ extracellular vesicles support pancreatic cancer aggressiveness.* J Clin Invest, 2016. **126**(11): p. 4140-4156.

192. Tobita, K., et al., *Thrombospondin-1 expression as a prognostic predictor of pancreatic ductal carcinoma.* Int J Oncol, 2002. **21**(6): p. 1189-95.

193. Adegoke, S.A., et al., *Thrombospondin-1 and Vitamin D in Children With Sickle Cell Anemia.* J Pediatr Hematol Oncol, 2019. **41**(8): p. e525-e529.

194. Amarasekera, A.T., et al., *Vitamin D supplementation lowers thrombospondin-1 levels and blood pressure in healthy adults.* PLoS One, 2017. **12**(5): p. e0174435.

195. Wu-Wong, J.R., M. Nakane, and J. Ma, *Vitamin D analogs modulate the expression of plasminogen activator inhibitor-1, thrombospondin-1 and thrombomodulin in human aortic smooth muscle cells.* J Vasc Res, 2007. **44**(1): p. 11-8.

196. Wu-Wong, J.R., et al., *Effects of Vitamin D analogs on gene expression profiling in human coronary artery smooth muscle cells.* Atherosclerosis, 2006. **186**(1): p. 20-8.

197. Garcia-Quiroz, J., et al., *Calcitriol reduces thrombospondin-1 and increases vascular endothelial growth factor in breast cancer cells: implications for tumor angiogenesis.* J Steroid Biochem Mol Biol, 2014. **144 Pt A**: p. 215-22.

198. Pal, S.K., et al., *THBS1 is induced by TGFB1 in the cancer stroma and promotes invasion of oral squamous cell carcinoma.* J Oral Pathol Med, 2016. **45**(10): p. 730-739.

199. Huang, T., et al., *FGF7/FGFR2 signal promotes invasion and migration in human gastric cancer through upregulation of thrombospondin-1.* Int J Oncol, 2017. **50**(5): p. 1501-1512.

200. Daubon, T., et al., *Deciphering the complex role of thrombospondin-1 in glioblastoma development.* Nat Commun, 2019. **10**(1): p. 1146.

201. Jeanne, A., et al., *Matricellular TSP-1 as a target of interest for impeding melanoma spreading: towards a therapeutic use for TAX2 peptide.* Clin Exp Metastasis, 2016. **33**(7): p. 637-49.

202. Okada, K., et al., *Stromal thrombospondin-1 expression is a prognostic indicator and a new marker of invasiveness in intraductal papillary-mucinous neoplasm of the pancreas.* Biomed Res, 2010. **31**(1): p. 13-9.

203. Albo, D., D.H. Berger, and G.P. Tuszynski, *The effect of thrombospondin-1 and TGF-beta 1 on pancreatic cancer cell invasion.* J Surg Res, 1998. **76**(1): p. 86-90.

204. Jeanne, A., et al., *Identification of TAX2 peptide as a new unpredicted anti-cancer agent.* Oncotarget, 2015. **6**(20): p. 17981-8000.

205. Pan, Y., et al., *Single-cell RNA sequencing reveals compartmental remodeling of tumor-infiltrating immune cells induced by anti-CD47 targeting in pancreatic cancer.* J Hematol Oncol, 2019. **12**(1): p. 124.

206. Golubovskaya, V., et al., *CD47-CAR-T Cells Effectively Kill Target Cancer Cells and Block Pancreatic Tumor Growth.* Cancers (Basel), 2017. **9**(10).

207. Cioffi, M., et al., *Inhibition of CD47 Effectively Targets Pancreatic Cancer Stem Cells via Dual Mechanisms.* Clin Cancer Res, 2015. **21**(10): p. 2325-37.

IV. Acknowledgment

To begin with, I would like to show great appreciation to Prof. Dr. Alexandr Bazhin from Ludwig-Maximilians-Universität München, who has offered great help to me and given lots of precious advice in the progress of my project. Additionally, his rich knowledge and rigorous logical thinking in scientific research have impressed me greatly and set an excellent example for me in my scientific research in the future.

Furthermore, I hope to acknowledge my supervisor, PD Dr. med. Jan G. D'Haese for his continuous support in my research. From the topic selection to the implementation of the research plan, this project has been finished under his careful supervision. Also, he offered me many chances to participate in some international forums, such as the World Pancreas Forum, European Pancreas Club meeting, and Deutsch Pancreas Club meeting, which help me meet many experts in the field of pancreas research.

Besides, I would like to thank the colleagues of our laboratory biobank, Maresa Demmel, Dennis Nothdurft, and Tommi Bauer, who have helped a lot in my study, thereby making my project progress well.

Additionally, I want to thank other doctorate candidates in our group, Yang Wu, Zhiqiang Li, and Quan Li. They have given me lots of excellent suggestions and support for my project.

My sincere appreciation goes to my parents Yinhai Zhang and Zhimei Ju, my husband, Yang Wu. They always give me enough support and trust and encourage me when I face difficulties.

Finally, I sincerely thank my doctor father, Prof. Dr. med. Jens Werner, who gives me this valuable opportunity to study as a doctorate candidate at LMU. During the three

years, I have met many wonderful persons, experienced different cultures, and paid visits to many fascinating places, which is an extraordinary and unforgettable experience for me.